7-1964

Angular correlation of CO^{60}

Henry Kuhlman

ANGULAR CORRELATION OF Co^{60}

by

Henry Kuhlman

A thesis presented to the
Faculty of the School of Graduate
Studies in partial fulfillment
of the
Degree of Master of Arts

Western Michigan University
Kalamazoo, Michigan
July 1964

ACKNOWLEDGEMENTS

The author wishes to express his sincere gratitude to Dr. George Bradley for his guidance and advice during every phase of this project. A word of thanks also is given to Dr. Larry Oppliger and Mr. Gus Hoyer for their stimulating discussions and consultations.

Especially the author thanks his wife, Pat. He is indebted to her not only for the typing and preparation of the manuscript but also for her endurance and encouragement during the many months of data taking.

Henry Kuhlman

TABLE OF CONTENTS

CHAPTER PAGE

TABLE OF FIGURES

CHAPTER I

INTRODUCTION

The probability that a radioactive nucleus will emit a gamma ray may depend on the angle between the nuclear spin axis and the direction of emission. The radiation pattern of a sample of randomly oriented nuclei is isotropic. An anisotropic pattern may be observed if the nuclear spin axes are aligned.

Method of measurement. Rather than aligning the spin axes, one can sometimes select preferentially for measurement only those spins which are nearly aligned. This selection is possible if a nucleus decays by two successive radiations R_1 and R_2. Choosing a fixed direction of emission to detect R_1 selects an ensemble of nuclei which has an anisotropic distribution of spin orientations. The direction in which R_2 is emitted then shows a definite angular correlation with respect to the chosen fixed direction used to detect R_1.

To measure an angular correlation, one must have a nucleus which emits two particles or gamma rays in rapid succession. Experimentally one records the number of coincidences between the two particles or gamma rays as a function of the angle between the two directions of propagation. This relationship between the coincidence counting rate and the angle between the directions of propagation is defined as the correlation function $W(\theta)$.

Expansion of the correlation function. $W(\theta)$ has been calculated theoretically for all cases involving gamma ray cascades. The correlation function can be expanded as a sum of Legendre polynomials; viz., $W(\theta) = \sum_{n=0}^{n_{max}} A_n P_n(\cos\theta)$. Since the positive θ direction is arbitrarily chosen, $W(\theta)$ must equal $W(-\theta)$; i.e., $W(\theta)$ is an even function. This shows that only even Legendre polynomials need be included in the expansion; i.e., in the above expansion, all n's are even integers.

In the case in which two gamma rays are emitted, three nuclear states must be involved. Let the three states (initial, intermediate, and final) be designated by A, B, and C respectively. The angular momenta of the nuclear levels may be designated by $\bar{I}_A$, $\bar{I}_B$, and $\bar{I}_C$ and the angular momenta of the gamma rays by $\bar{L}_1$ and $\bar{L}_2$ respectively. For conservation of angular momentum to be satisfied, the following equations must be satisfied; $\bar{I}_A = \bar{I}_B + \bar{L}_1$ and $\bar{I}_B = \bar{I}_C + \bar{L}_2$. Two gamma rays in being emitted from a nucleus can be characterized by the angular momentum quantum numbers or multipolarities L_1 and L_2. The correspondence between $\bar{L}_1$ and L_1 is given by $\bar{L}_1 \cdot \bar{L}_1 = L_1(L_1+1)\hbar^2$ and similarly $\bar{L}_2 \cdot \bar{L}_2 = L_2(L_2+1)\hbar^2$. The nuclear levels have associated angular momentum quantum numbers I_A, I_B, and I_C, which are related to $\bar{I}_A$, $\bar{I}_B$, and $\bar{I}_C$ by the following: $\bar{I}_A \cdot \bar{I}_A = I_A(I_A+1)\hbar^2$, $\bar{I}_B \cdot \bar{I}_B = I_B(I_B+1)\hbar^2$, and $\bar{I}_C \cdot \bar{I}_C = I_C(I_C+1)\hbar^2$.

The highest order term in the Legendre expansion of the correlation function is given by $n_{max} = \text{Min}(2I_B, 2L_1, 2L_2)$. The

half-life of an excited nuclear state is dependent upon the energy and multipolarity of the gamma ray emitted. Energies which normally are available in radioactive decays are such that multipolarities less than 2 possess half-lifes of greater than 10^{-6} seconds. Experimentally it is impossible to measure the directional correlation function of a cascade involving an intermediate state with so long a half-life. Therefore most correlation functions which can be investigated experimentally are given by the following:

$$W(\theta) = 1+A_2P_2(\cos\theta)+A_4P_4(\cos\theta).$$

Dependence of the coefficients. The coefficients A_2 and A_4 depend on the following five parameters: the multipole orders L_1 and L_2 of the gamma rays and the spins I_A, I_B, and I_C of the nuclear states. Specifically $A_n = F_n(L_1I_AI_B)F_n(L_2I_CI_B)$ where the $F_n(LI_iI_j)$ have been theoretically calculated and tabulated.[1] The results of an angular correlation experiment alone will therefore never allow a complete determination of all of the nuclear parameters involved. Only in conjunction with other experiments is it possible to establish a complete decay scheme. The angular correlation function $W(\theta)$ does not depend on the parities of the nuclear states. Thus it is impossible to distinguish between electric and magnetic radiation by means of an angular correlation experiment.

---

[1] L. C. Biedenharn and M. E. Rose, Reviews of Modern Physics, Vol. 25, p. 3, (1953).

CHAPTER II

THE PROBLEM AND GAMMA RAY DETECTION

I. The Problem

Decay scheme of Co^{60}. Co^{60} nuclei are radioactive with a half-life of 5.24 years. Their mode of de-excitation is by the emission of a beta particle. After the emission of the beta particle, the nucleus is in an excited state of Ni^{60}. The mode of de-excitation for the Ni^{60} nuclei is by the emission of two gamma rays in cascade. The high energy crossover gamma ray from the highest level to the lowest level is highly forbidden by the selection rules and has not been observed. Fig. 1 is the most probable decay scheme of Co^{60}.[2,3]

---

[2]K. Way, et. al., "Nuclear Level Schemes," A = 20 - A = 92 Atomic Energy Comission Report TID-5300, (1955).

[3]J. R. Bell, and P. R. Cheever, Nucleonics, Vol. 21, p. 58, (July 1963).

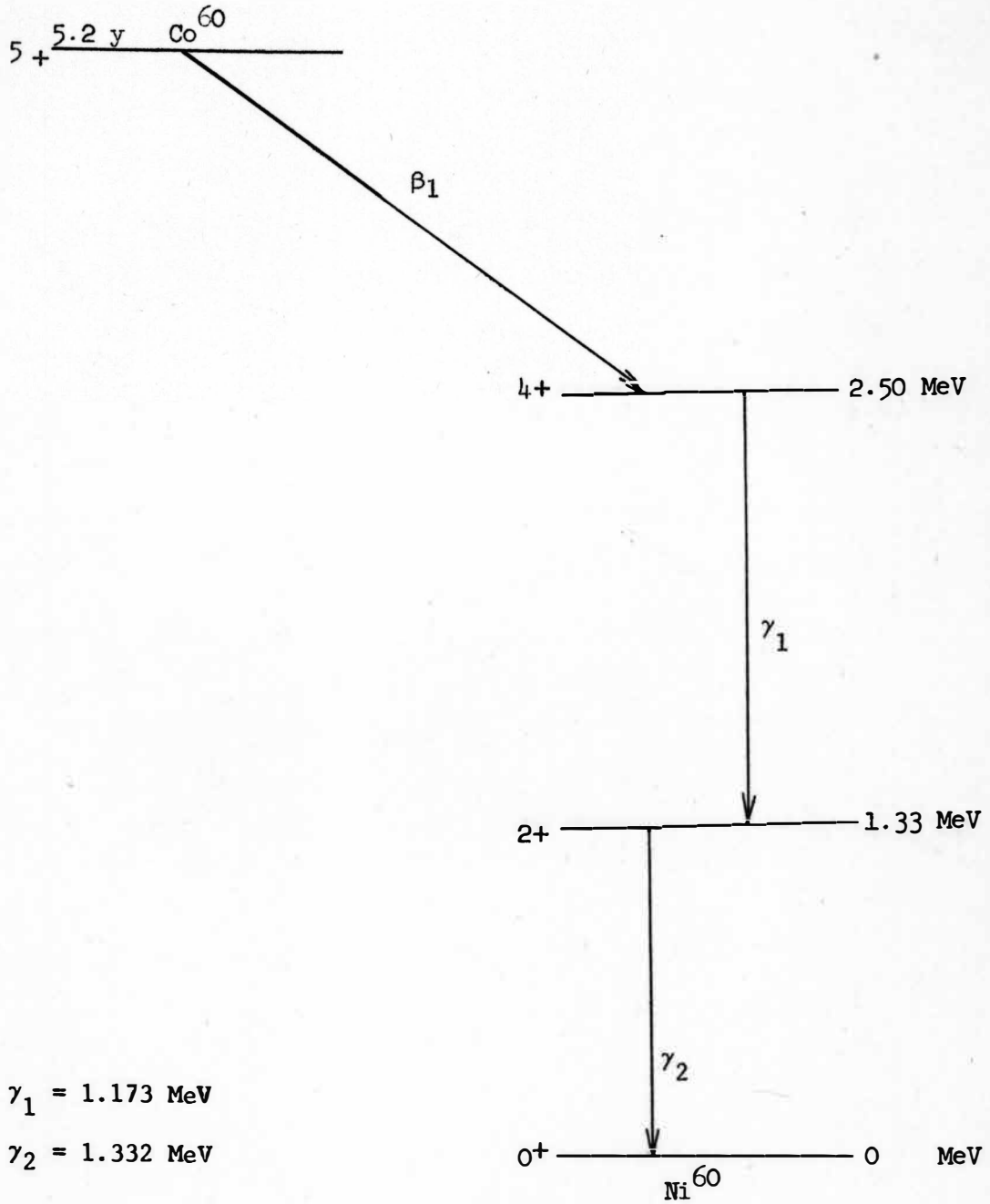

Fig. 1. Decay scheme of Co^{60}.

Possibility of measurement. Since the half-life of the intermediate state is less than 10^{-12} seconds (S), a coincidence circuit with a resolving time of 10^{-6} S will sense pulses from the two photons as being simultaneous. With the half-life of the intermediate state being less than 10^{-12} S, the nucleus is not realigned by precession or thermal vibrations between the times of emission of the two gamma rays. If the half-life of the intermediate state were greater than 10^{-8} S, it would be possible for the nucleus to partially lose alignment due to extranuclear interactions. This would make measurements of the angular correlation function extremely difficult, if not impossible.

Statement of the problem. The object of this experiment was to investigate the angular dependence between the directions of γ_1 and γ_2; i.e., to determine $W(\theta)$. To find this angular dependence, an arbitrary direction is chosen to detect one of the gamma rays, and then a measurement is made of the counting rate of all gamma rays in coincidence with it as a function of the angle between the two detectors.

II. Detection of Gamma Rays

Description of NaI(Tl) detectors. The use of thallium activated sodium iodide scintillation crystals mounted on photomultiplier tubes is the most efficient method of detecting gamma rays and gives the best energy resolution. NaI(Tl) crystals convert gamma rays to visible light pulses whose intensity is directly proportional to

the energy given up by the gamma ray while in the crystal. This burst of visible light is then converted by the photomultiplier tube into an electrical signal whose amplitude is thus directly proportional to the energy that the incoming gamma ray lost in the crystal. Fig. 2 is a diagram of a NaI(Tl) crystal mounted on a photomultiplier tube.

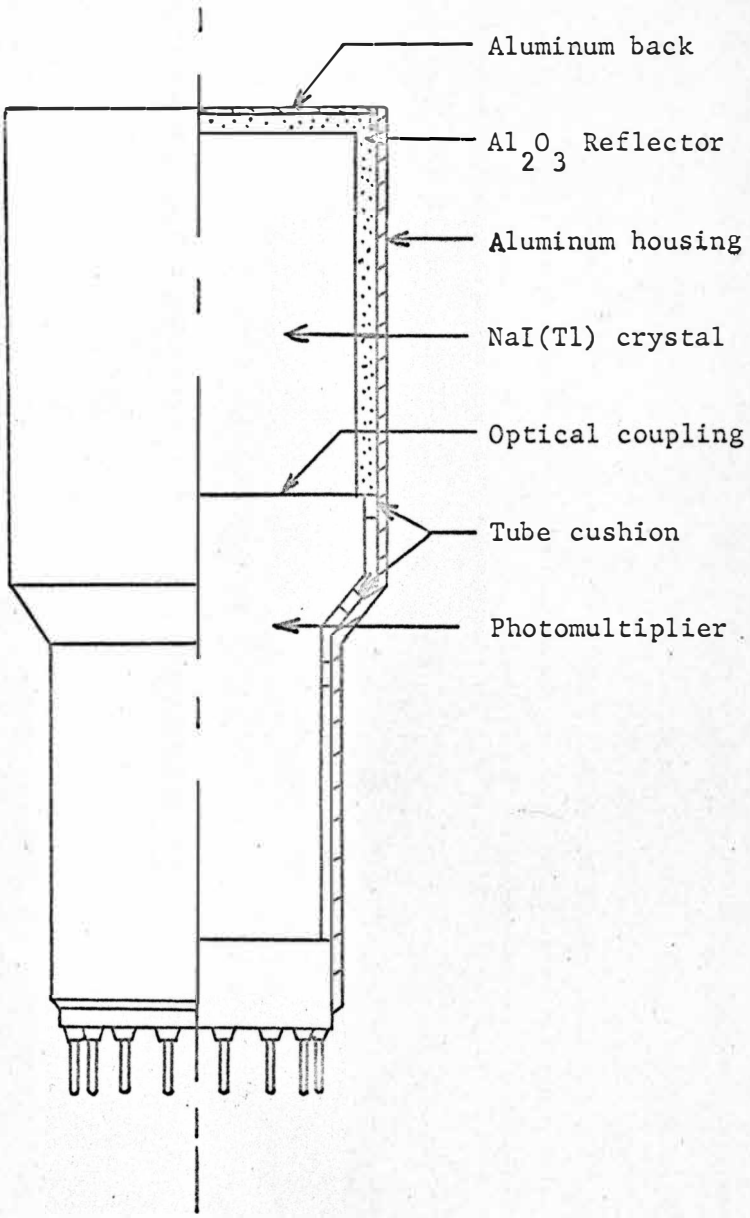

Fig. 2

Photomultiplier tube output signals. The electrical signals from the photomultiplier tube can be viewed on an oscilloscope and have the shape as pictured in Fig. 3. These signals can be fed directly into a scaler and counted; however, it is more useful to sort them according to pulse height and store them in a multi-channel analyzer.

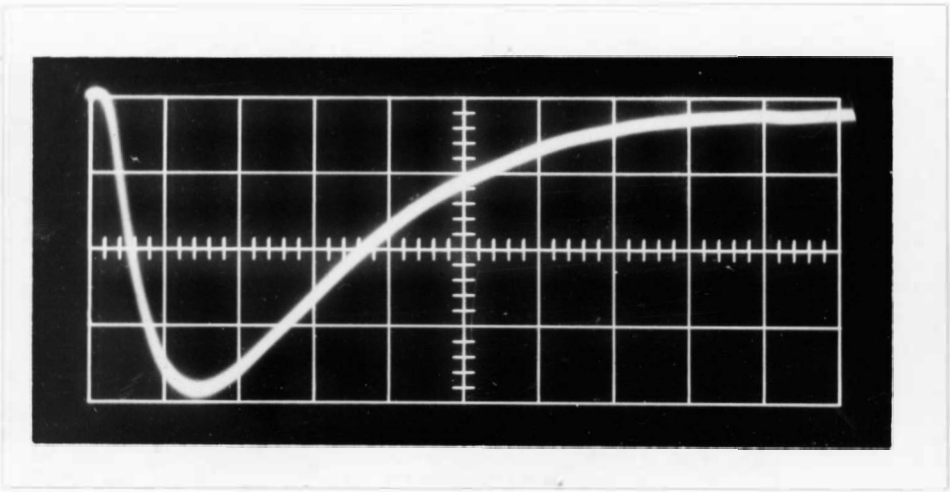

On the abscissa the scale is 0.5 μs per cm.

On the ordinate the scale is 5.0 mV per cm.

Note that the signals are negative; i.e., the top grid line represents zero voltage.

Fig. 3. Output signals from a photomultiplier tube.

III. Interpretation of a Gamma Ray Spectrum

Interactions of gamma rays. Gamma rays interact with matter in three ways: photoelectric effect, Compton effect, and pair production. Any combination of processes by which the total energy of the gamma ray is completely absorbed in the crystal will produce pulses of approximately the same height. If a gamma ray interacts with an electron in the crystal by means of the Compton effect and the scattered photon escapes the crystal, an electrical pulse will still be produced. However, the height of this pulse will correspond in energy to the difference between the energy of the incident gamma ray and the energy of the scattered gamma ray. The absorption coefficient for pair production in the 1.17 to 1.33 MeV energy range is very small; therefore the number of electron positron pairs created is small.

Decay scheme of Cs^{137}. A group of monoenergetic gamma rays has a characteristic shape when recorded by a multichannel analyzer. As an example of this characteristic shape, a spectrum of Cs^{137} will be considered. Cs^{137} is radioactive and decays by the emission of a beta particle. The half-life for this decay is 27 years. The amount of energy that is carried off in this beta emission transforms the Cs^{137} nucleus to an excited state of Ba^{137}. This isomeric state of Ba^{137} decays to the ground state of Ba^{137} by the emission of a 0.662 MeV gamma ray. A 0.032 MeV X-ray is also produced by an electron which enters the K shell following the ejection of an

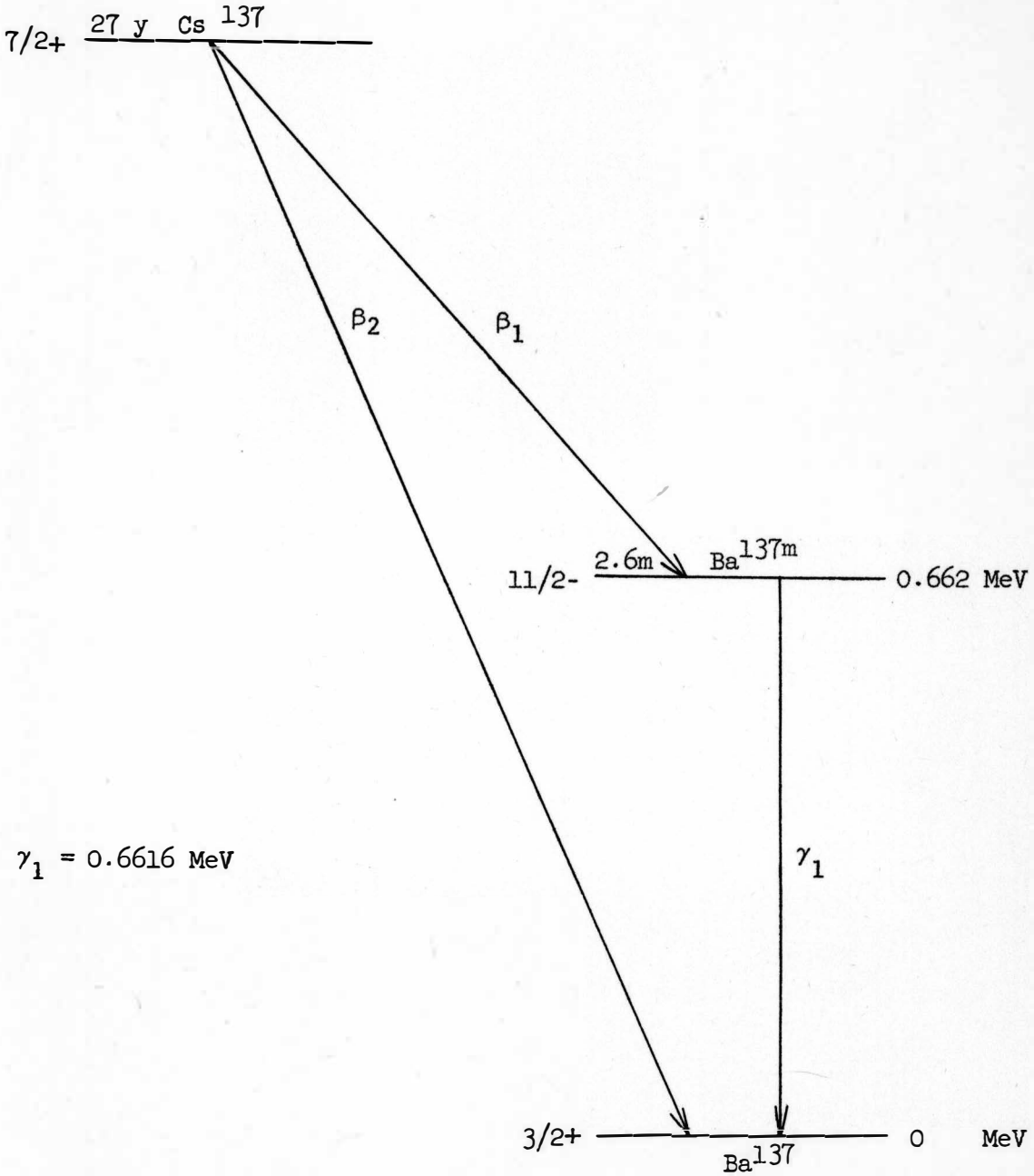

Fig. 4. Decay scheme of Cs^{137}.

electron from this shell by internal conversion. Fig. 4 is the decay scheme of Cs^{137}.[4,5]

The interpretation of the Cs^{137} spectrum. A spectrum of Cs^{137} is displayed in Fig. 5. The different portions of the spectrum are interpreted as follows.

(a) This line represents the Barium X-ray, and corresponds in energy to 0.032 MeV. This peak can be removed from the spectrum by inserting a thin absorber between the source and the detector.

(b) This broad portion of the spectrum is caused by gamma rays which scatter from the crystal giving up only a fraction of their energy.

(c) This edge corresponds to a Compton scattering in which the gamma loses the maximum energy possible. This is called the Compton edge.

(d) This peak represents the photoelectric peak corresponding to an energy of 0.662 MeV. The reason for the rather large spread in energy is that the number of photons emitted per gamma ray and collected in the photomultiplier tube is a statistical process. Also the number of electrons emitted by the photomultiplier phosphor upon bombardment by the flash of visible light is a statistical process.

---

[4] M. A. Waggoner, Physical Review, Vol. 82, p. 906, (1951).

[5] Nuclear Data Sheets, Vol. 2, (1961).

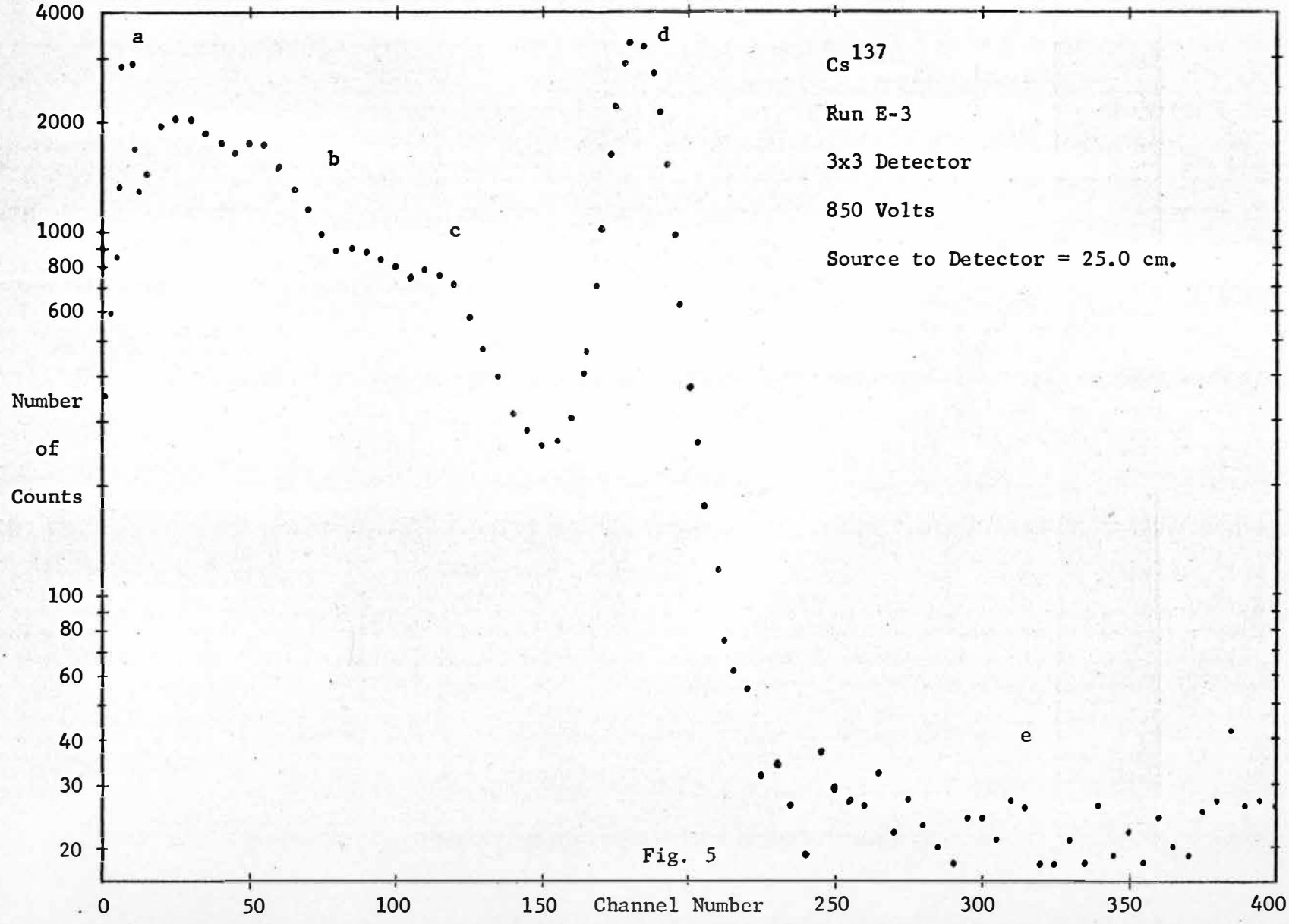
4000
2000
1000
800
600
100
80
60
40
30
20
a
b
c
d
e
Cs137
Run E-3
3x3 Detector
850 Volts
Source to Detector = 25.0 cm.
Number
of
Counts
0
50
100
150
Channel Number
250
300
350
400

Fig. 5

(e) Counts appearing in this region represent pile-up. A sum of two pulses is recorded in this region of the spectrum when two pulses are created simultaneously. At higher counting rates, this region of the spectrum becomes more pronounced.

The interpretation of the Co^{60} spectrum. The Co^{60} spectrum as pictured in Fig. 6 is similar to the Cs^{137} spectrum except in the following regions.

(A) There is no low energy X-ray in the decay process of Co^{60}, since its internal conversion coefficient is very small.

(B) This peak is due to a backscattering. It is caused by the detection of gamma rays which are Compton scattered at 180^{o} from the other detector which was located directly across the sample from the detector used to record this spectrum.

(C) The lower energy photopeak corresponds in energy to 1.17 MeV which is the energy of the γ_1 transition in the Ni^{60} cascade.

(D) The higher energy photopeak corresponds in energy to 1.33 MeV which is the energy of the γ_2 transition in the Ni^{60} cascade.

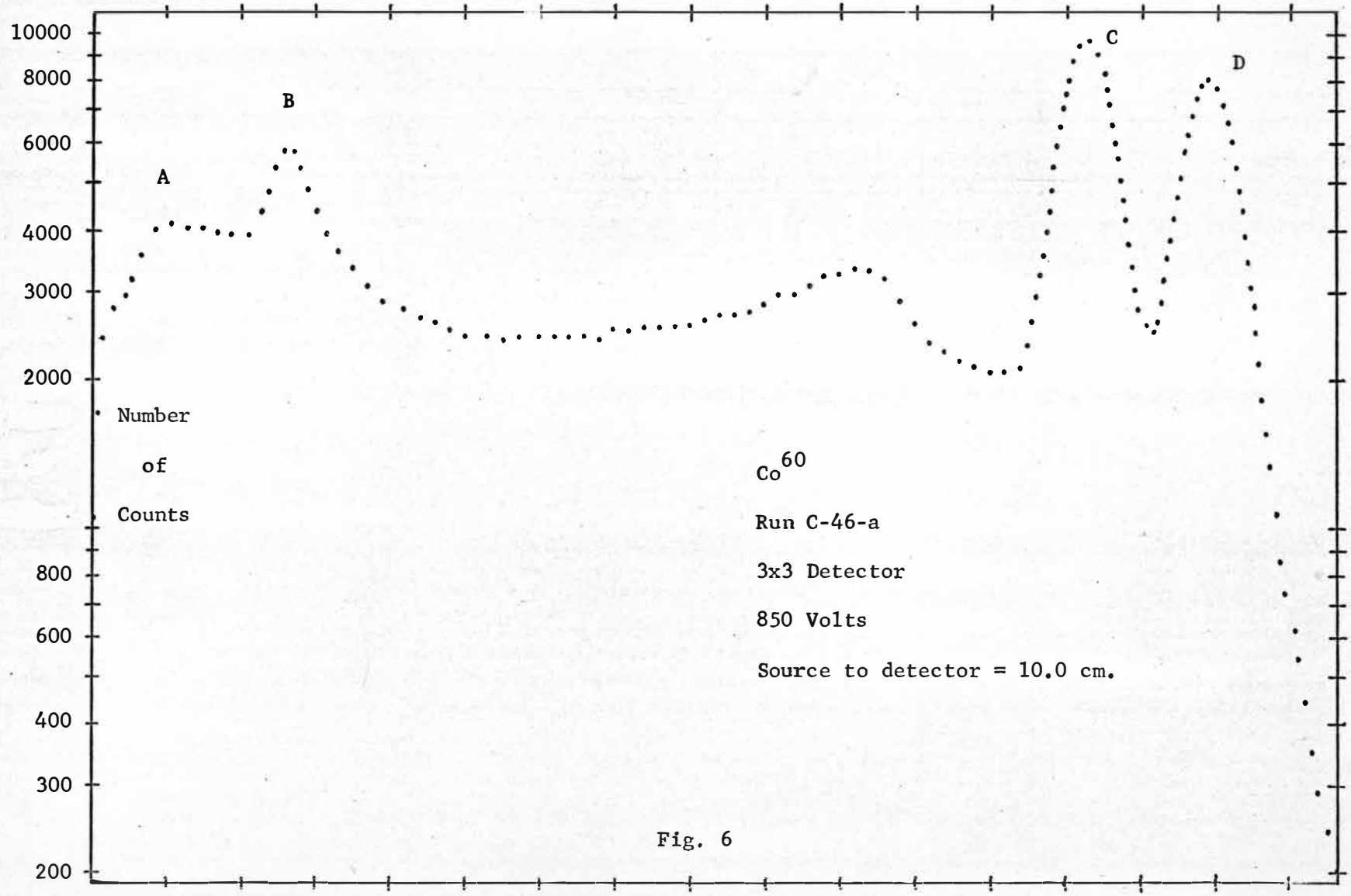
10000
8000
6000
4000
3000
2000
800
600
400
300
200
A
B
C
D
Number
of
Counts
Co^{60}
Run C-46-a
3x3 Detector
850 Volts
Source to detector = 10.0 cm.
0
50
100
150
Channel Number
250
300
350
400

Fig. 6

CHAPTER III

EXPERIMENTAL APPARATUS

A block diagram of the main components used in this experiment is shown in Fig. 7. A drawing of the angular correlation table with the two mounted detectors and the source is shown in Fig. 8.

Source. The Co^{60} source was in the form of $CoCl_2$ in a 1 normal solution of HCl. A 2 mC sample was purchased from Oak Ridge National Laboratory.[6] The Co^{60} was produced by neutron bombardment of Co^{59}, its concentration was greater than 1 mC per ml, and its specific activity was approximately 25,000 mC per gram of Co. The radio-active decay of impurities in the sample was less than 1% of the activity of the Co^{60}. A portion of the 2 mC sample was diluted with H_2O, and small amounts were placed in small test tubes. This made available various sources of Co^{60} radiation in strengths of from 3 μC to 100 μC.

In angular correlation measurements, the assumption is made that the source is a point source. This assumption was nearly satisfied in this case since the dimensions of the source were about 1 mm on each side, and the source to detector distances were 6.0 cm and 10.0 cm. The source was mounted on a movable pedestal

---

[6] Oak Ridge National Laboratory, Oak Ridge, Tennessee.

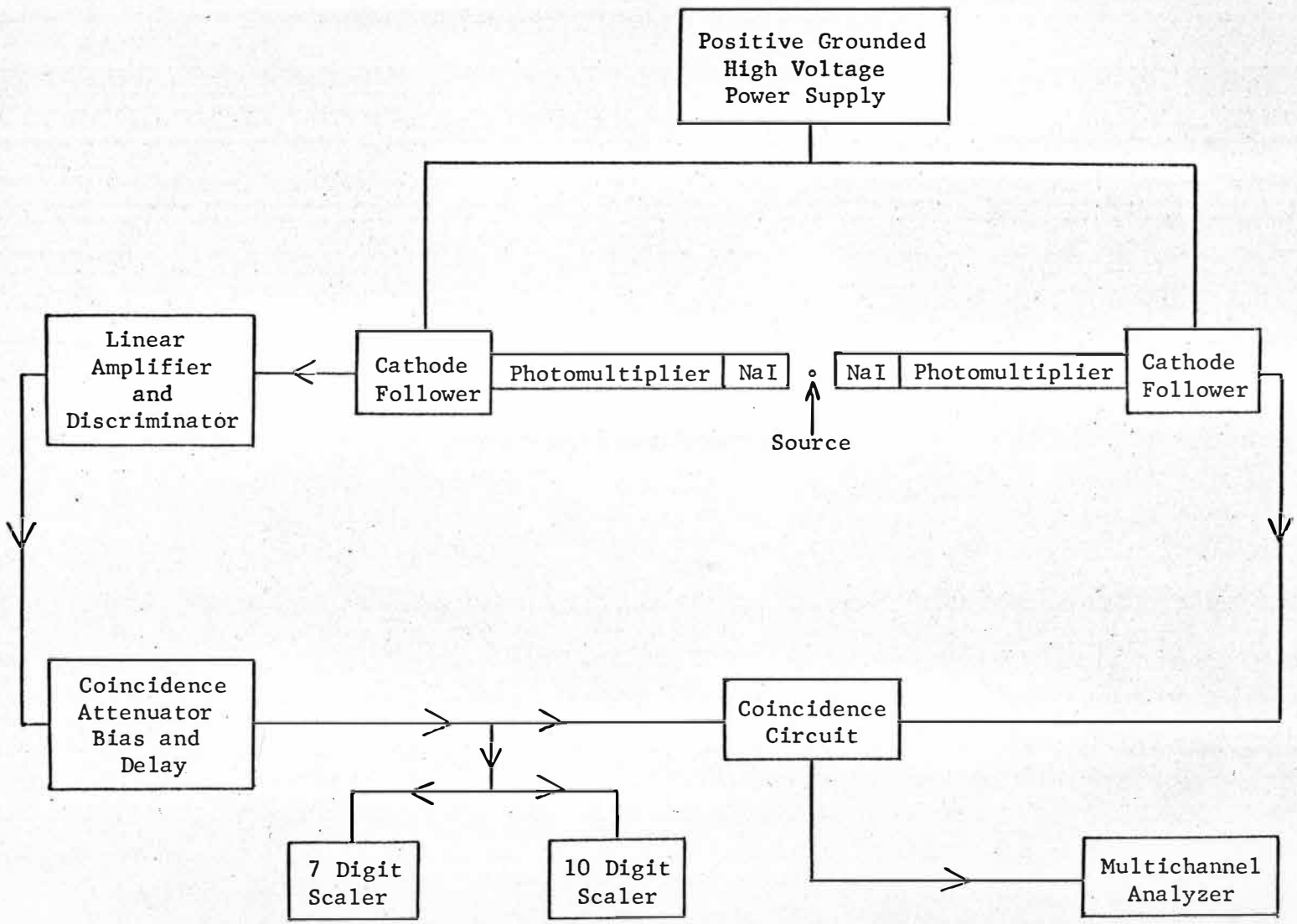
Positive Grounded
High Voltage
Power Supply
Linear
Amplifier
and
Discriminator
Cathode
Follower
Photomultiplier
NaI
NaI
Photomultiplier
Cathode
Follower
Source
Coincidence
Attenuator
Bias and
Delay
Coincidence
Circuit
7 Digit
Scaler
10 Digit
Scaler
Multichannel
Analyzer

Fig. 7.

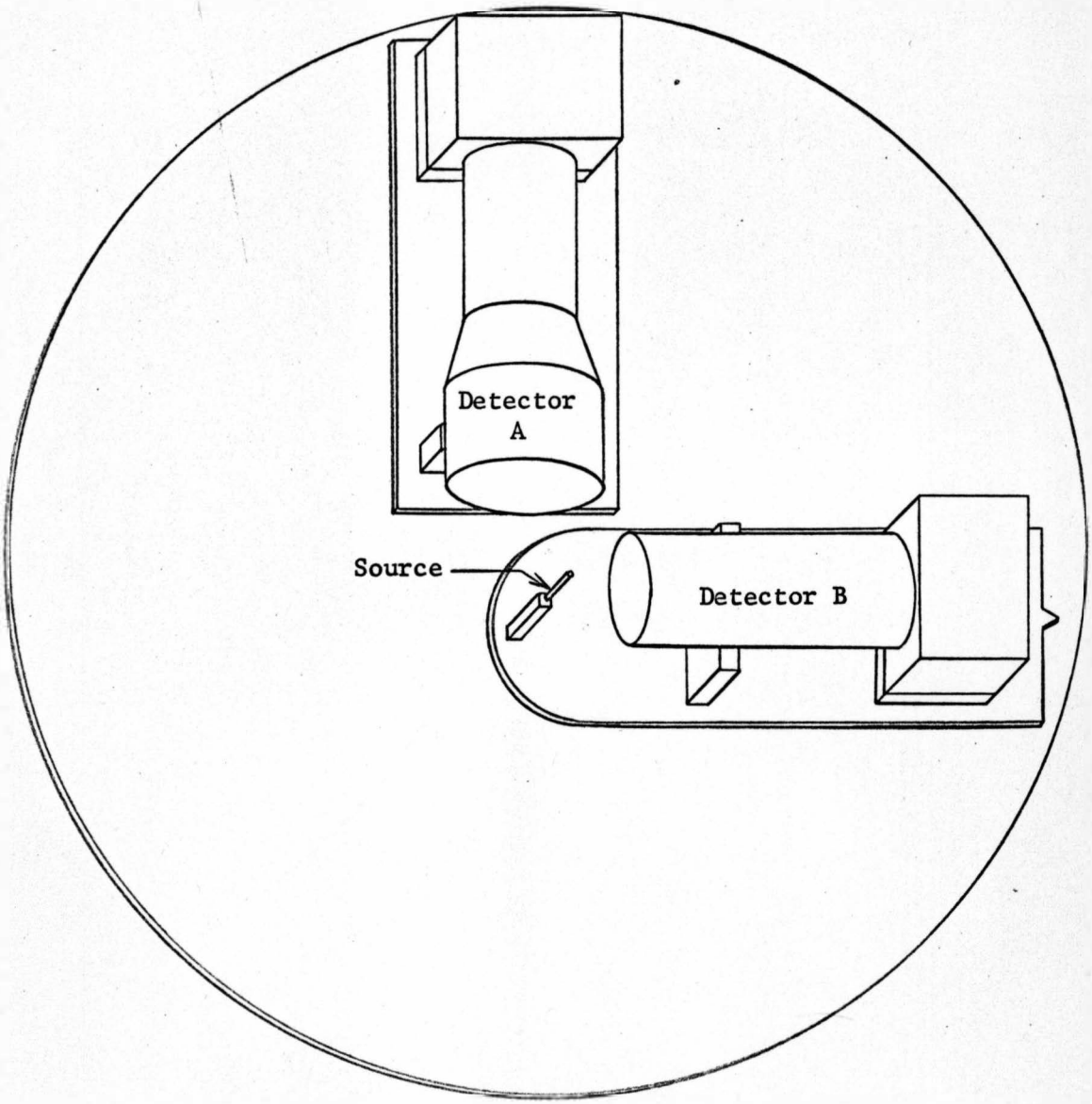

Fig. 8. Angular correlation table.

8.7 cm above the table. It was raised above the table to minimize the number of gamma rays that could scatter from the table and reach the detector.

Detector A. A 3x3 (three inches in diameter by three inches long, cylindrical shaped) NaI(Tl) crystal was used to detect the gamma rays. This crystal was matched to a 6363 Dumont[7] photomultiplier tube and together they were mounted in an aluminum jacket by the manufacturer, Isomet Corporation.[8] The detector was mounted on an angular correlation table with its front surface 10.0 cm from the source. The common axis of the photomultiplier tube and the crystal was parallel to the plane of the table, 8.7 cm above the table, and intersected the center of the source. The source was on the axis of the detector and 8.7 cm above the table.

The absolute efficiency of detection of a scintillation crystal depends upon the following parameters: crystal size, crystal composition, source to detector distance, and energy of gamma radiation. The calculated efficiency of a 3x3 NaI(Tl) crystal at 10.0 cm for gamma rays in the energy range 1.17 to 1.33 MeV is 1.7%.[9] This means that for every 1000 gamma rays that leave the source, 17 interact with the crystal.

---

[7]Allen B. Dumont Laboratories, Passaic, New Jersey.

[8]Isomet Corporation, Palisades Park, New Jersey.

[9]E. A. Wolicki, et. al., "Calculated Efficiencies of NaI Crystals," U. S. Naval Research Laboratory Report NRL-4833, (1956).

A measure of the quality of a gamma ray detector is its resolution. The resolution of a NaI(Tl) crystal is defined as the ratio of the full width of the Cs^{137} 0.662 MeV photopeak at half maximum to the position of the midpoint of the same peak. The resolution of the 3x3 detector used in this experiment was determined to be 9.5%.

Detector B. A 2x2 (two inches in diameter by two inches long, cylindrical shaped) NaI(Tl) crystal was used as the second detector. This crystal was manufactured by Harshaw Chemical Company[10] and was matched to a 6292 Dumont photomultiplier tube. The crystal and phototube were mounted on a movable carriage on the angular correlation table. The carriage was movable in the θ direction only. No provision was made for movement in the radial direction. The front surface of the 2x2 crystal remained 6.0 cm from the source. The common axis of the detector and the photomultiplier tube was parallel to the plane of the table, 8.7 cm above the table, and intersected the center of the source. The source was located on the axes of each of the detectors and on the axis of rotation of the 2x2 crystal.

The calculated absolute efficiency of a 2x2 NaI(Tl) crystal at 6.0 cm for gamma rays in the energy range 1.17 to 1.33 MeV is 1.2%.[9] The resolution of this crystal was experimentally determined to be 9.6%.

---

[10]The Harshaw Chemical Company, Cleveland, Ohio.

[9]E. A. Wolicki, et. al., "Calculated Efficiencies of NaI Crystals," U. S. Naval Research Laboratory Report NRL-4833, (1956).

The outputs from the photomultiplier tubes were connected to cathode followers in order to reduce the effects of the capacitance in the output cables.

Power supply. A positive grounded regulated power supply was used to supply the high voltage to the two photomultiplier tubes. The power supply used was a model RE-3002 manufactured by Northeast Scientific Corporation.[11] The output was voltage regulated to better than 0.005%. The long term stability was better than 0.01% per hour or 0.1% per day with a reasonably constant ambient temperature.

The gain of a photomultiplier tube is approximately proportional to the seventh power of the voltage across it. Therefore, for the gain to remain constant, the high voltage must be closely regulated. The 6363 and 6292 phototubes were both operated at 850 volts which was well below their rated maximum of 1800 volts from cathode to anode.

Discriminator. A Hamner[12] N-302 linear amplifier and differential pulse height discriminator were used to produce the coincidence signals. A N-302 has two components--a non-overloading linear amplifier incorporating both delay line and RC clipping, and a single-channel pulse height analyzer.

---

[11] Northeast Scientific Corporation, Acton, Massachusetts.

[12] Hamner Electronics Company, Inc., Princeton, New Jersey.

The signals from the 2x2 movable crystal were amplified and passed to the differential discriminator portion of the circuit which selected the pulses in a particular pulse height range. If a pulse fell between E and E+ΔE, the discriminator generated an output pulse of constant shape. Both E and ΔE were continuously variable by means of two ten-turn potentiometers.

The output signals from a N-302 are square with a height of 25 volts and a duration of 1.0 μs. By changing capacitor C-76 from 68 μμF to 118 μμF, they were lengthened to 1.2 μs; see Fig. 9. The resolving time of the pulse height analyzer was 1.3 μs.

Coincidence circuit. The coincidence circuit of the model ND-120 Nuclear Data[13] multichannel analyzer was used in this experiment. The circuit operates as follows. Access to the storage unit is blocked by applying a constant DC voltage of -3.0 volts to the coincidence input. Access to the storage unit is possible only while the coincidence input is at +1.0 volts.

It is important that the coincidence signal not be excessively long. However, the signals must be long enough to allow the signal pulses to reach their maxima and begin to decrease while access to the storage unit is available. Since the rise time of the signal pulses must be at least 0.7 μs to allow accurate storage, a width of 1.2 μs was chosen as the optimum length of the coincidence signals. The resolving time of the circuit was 1.2 μs.

---

[13]Nuclear Data, Inc., Madison, Wisconsin.

Analyzer. The multichannel pulse height analyzer which was used was a model ND-120 manufactured by Nuclear Data. This analyzer has the following main components: a linear amplifier, an analog to digital converter, a special purpose digital computer, and a number of individual single channel scalers. The model ND-120 analyzer has 512 channels.

Readout of the information stored in the pulse height analyzer was possible in three different ways. The number of counts in each of the 512 channels could be displayed on a cathode-ray tube, graphed on paper by an X-Y plotter, or typed on special sheets by a semi-automatic electric typewriter. Since for angular correlation measurements the number of counts in an energy interval must be known as accurately as possible, the stored information was extracted from the analyzer by instructing the analyzer to type out the information.

When the contents of the storage unit are typed out, the number of counts in each channel is displayed exactly. When the information is displayed on a cathode-ray tube or graphed by an X-Y plotter, the number of counts in a specific channel must be interpolated. Interpolation is satisfactory when the number of counts is small; however, for large numbers interpolation is very limited in precision.

Scaler. A scaler was used to count the number of coincidence signals produced by the discriminator. Since the number of coincidences recorded in each run was normalized to the number of times

the coincidence window opened, it was necessary to record precisely the number of signals generated by the discriminator. For this reason, two scalers were connected in parallel to serve as a check.

One of the counters had seven digits while the other was a ten digit instrument. Although the same pulses were delivered to each counter, the counters did not have identical counting rates; however, this was predictable. The counting rates were different because the seven digit scaler had a shorter resolving time than the ten digit unit. Two closely spaced coincidence signals would record as one on the ten digit counter while the seven digit one distinguished two separate pulses. It can be shown that the difference in counting rates between the two scalers is proportional to the square of the counting rate of the faster one. This proportionality was observed.

Coincidence signals. As viewed on an oscilloscope, the coincidence pulses generated by the discriminator had the shape pictured in Fig. 9.

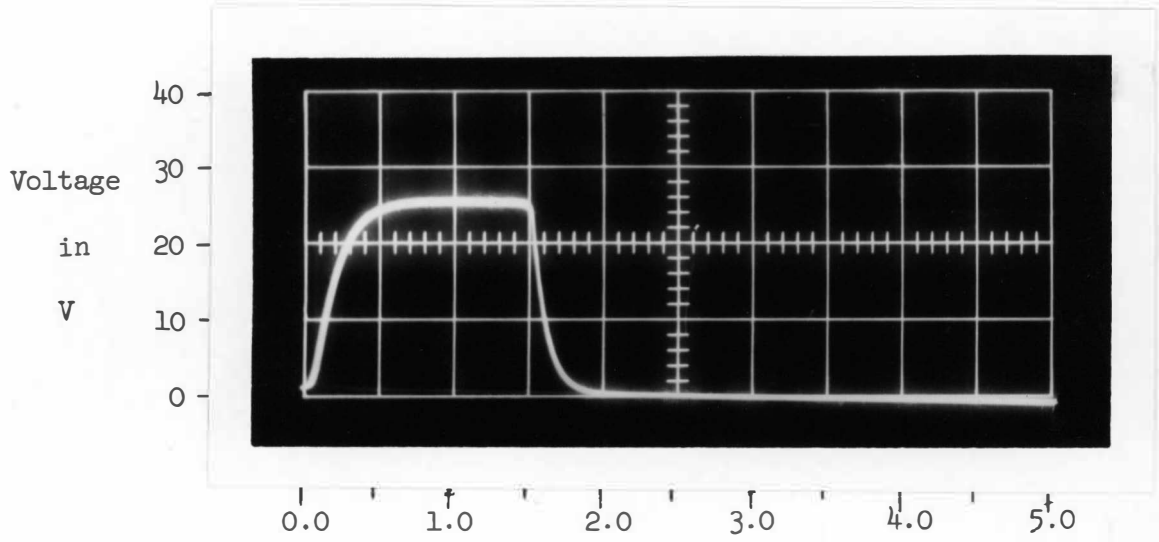

Fig. 9

After being attenuated and biased, the pulses appeared as in Fig. 10.

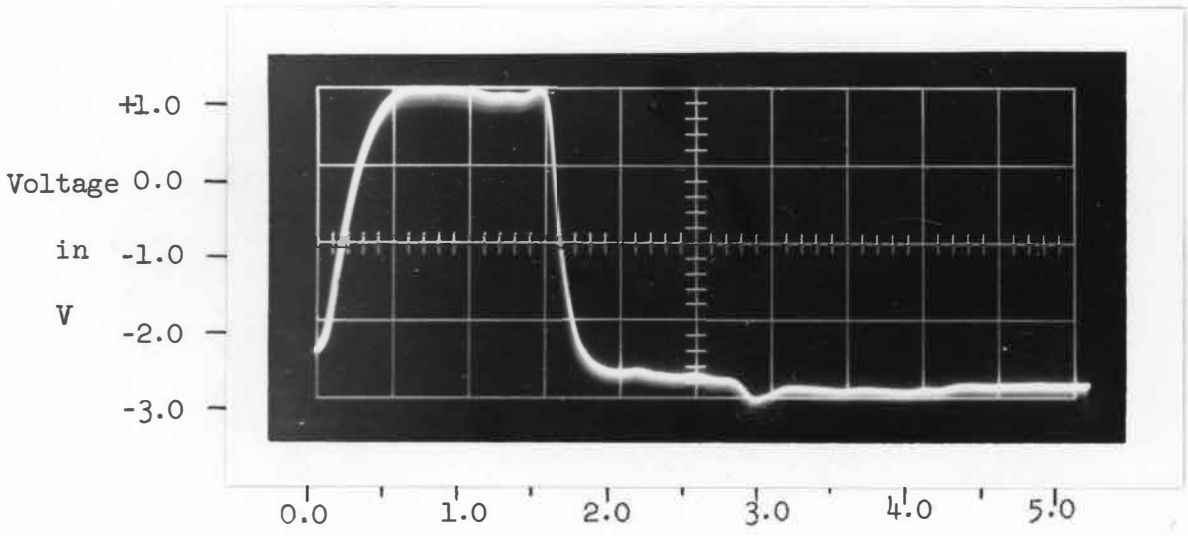

Fig. 10

Coincidence attenuator, bias, and delay. The multichannel analyzer delays all incoming signals by 2.0 μs before it stores them. This allows the discriminator 2.0 us to create the coincidence pulses. The Hamner N-302 discriminator required less than 2.0 μs to create the coincidence pulses after an incoming signal fell between E and E+ΔE. Therefore, the coincidence pulses had to be delayed before they arrived at the multichannel analyzer.

To facilitate this delay, a variable delay circuit was constructed. Since these same pulses also had to be attenuated and biased, these operations were incorporated in the same unit. Fig. 11 is a schematic diagram of the coincidence attenuator, bias, and variable delay. The signals were attenuated by means of a simple voltage divider. They were biased to -3.0 volts by an external battery. The delay line was variable in steps of 0.1 μs from 0.0 μs through 2.0 μs. The delay line was critically damped with 300 ohms which eliminated echoes.

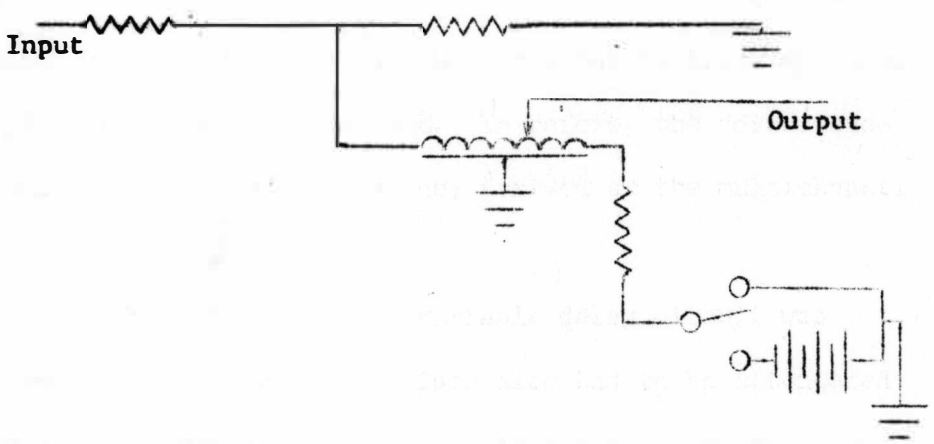

Fig. 11. Coincidence attenuator, bias, and delay.

To find the correct length of delay required, various delays were tried. Delays of 0.6, 0.7, and 0.8 μs allowed the photopeaks to be stored in a maximum channel while delays of longer or shorter duration would suppress the channel number; i.e., the photopeaks would fall in lower channels. It was concluded that with a delay of 0.7 μs the coincidence pulses would straddle in time the signals coming directly from the 3x3 stationary detector.

CHAPTER IV

EXPERIMENTAL PROCEDURE

I. Spectra

Coincidence window. An important preliminary adjustment was the setting of the coincidence window. It might be thought best to set the discriminator levels to just straddle the 1.33 MeV photopeak. This would give the spectrum in coincidence the shape of a monoenergetic gamma radiation of 1.17 MeV. The discriminator levels could also be set around the lower energy gamma thereby recording a coincidence spectrum of the 1.33 MeV gamma. It can be shown that setting the lower level in the valley of the 1.17 MeV gamma and the higher level on the high edge of the 1.33 MeV gamma is just as effective and much more efficient.

To set these levels, the signals from the 2x2 movable crystal were sent to both the discriminator and the multichannel analyzer. The levels were then adjusted until just the two photopeaks showed in a coincidence spectrum. The discriminator produced a coincidence pulse for each of the signals from the 2x2 crystal which fell between E and $E+\Delta E$. After being delayed, attenuated, and biased, these coincidence signals reached the coincidence circuit at the same time as their generating pulses

(the pulses from the 2x2 crystal). Since the pulses were in coincidence with themselves, the multichannel analyzer would record only the pulses which attained height E to E+ΔE since only they would be accompanied by a coincidence signal.

Fig. 12 is a spectrum of the signals falling between E and E+ΔE. The reason that there is no definite maximum is that pile-up is highly probable at these counting rates. With a source strength of 3.5 μC, there were about 70,000 coincidence pulses per minute. A source strength of 5.0 μC increased this to about 112,000 counts per minute.

The coincidence spectrum. With the window set as above, spectra were recorded. The following is an example of their photopeaks. Fig. 13 shows the photopeaks as recorded by the analyzer connected to the 3x3 stationary crystal with no coincidence. Fig. 14 displays the photopeaks of a coincidence spectrum.

Accidental coincidences. A spectrum of the accidental coincidences was obtained by setting the delay on the coincidence pulses at 0.0 μs and delaying the signals from the 3x3 by 1.0 μs. This insured that no true coincidences were recorded. Fig. 15 shows the photopeaks of an accidental coincidence spectrum.

It is clear that the coincidence spectra are different in shape from the spectrum taken with no coincidence. Pulses are stored in the channel corresponding to the maximum height of the pulse during the 1.2 μs that the window was open. The signals in

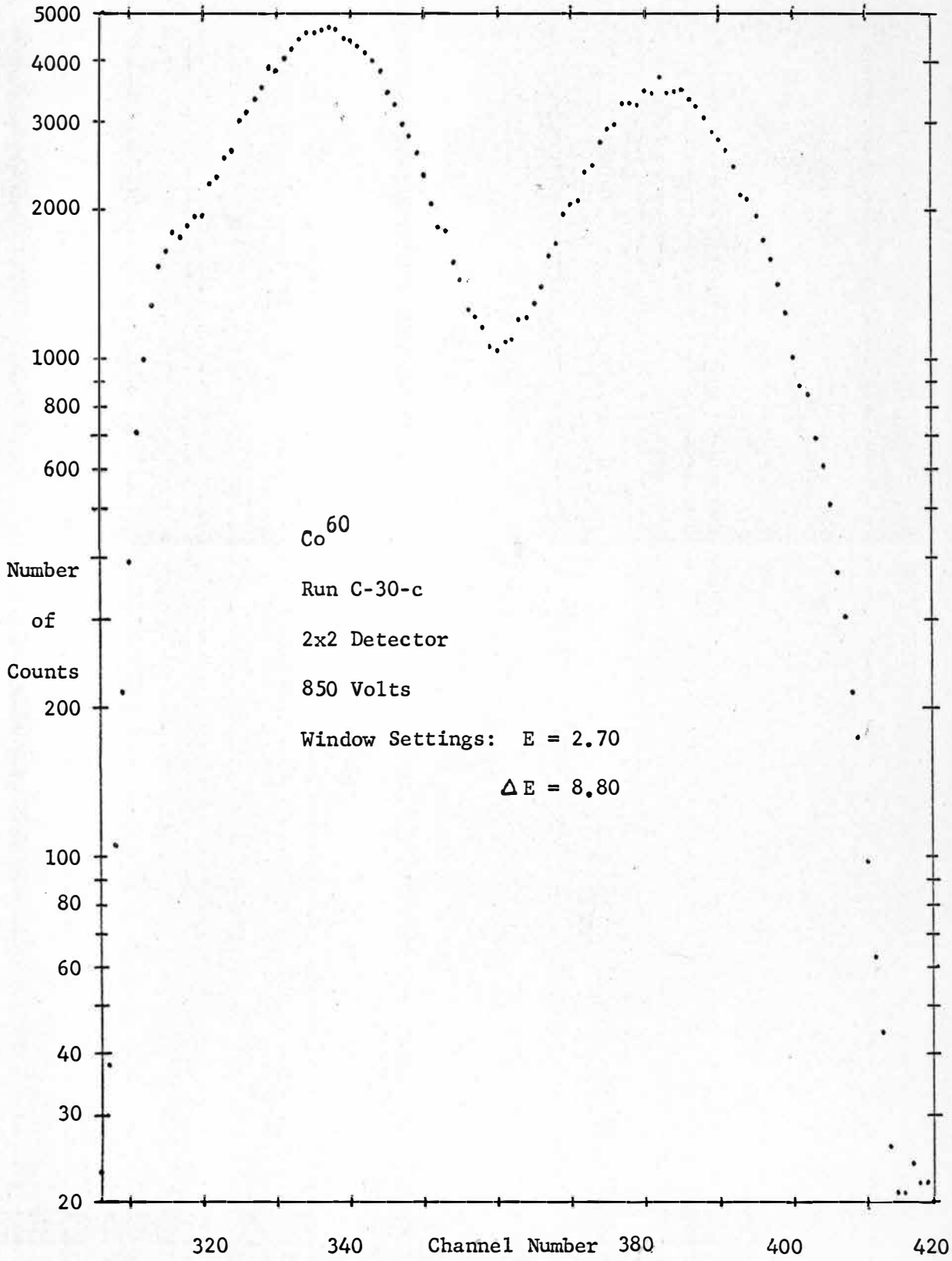
5000
4000
3000
2000
1000
800
600
200
100
80
60
40
30
20
Number of Counts
Co^{60}
Run C-30-c
2x2 Detector
850 Volts
Window Settings: E = 2.70
ΔE = 8.80
320
340
Channel Number
380
400
420

Fig. 12

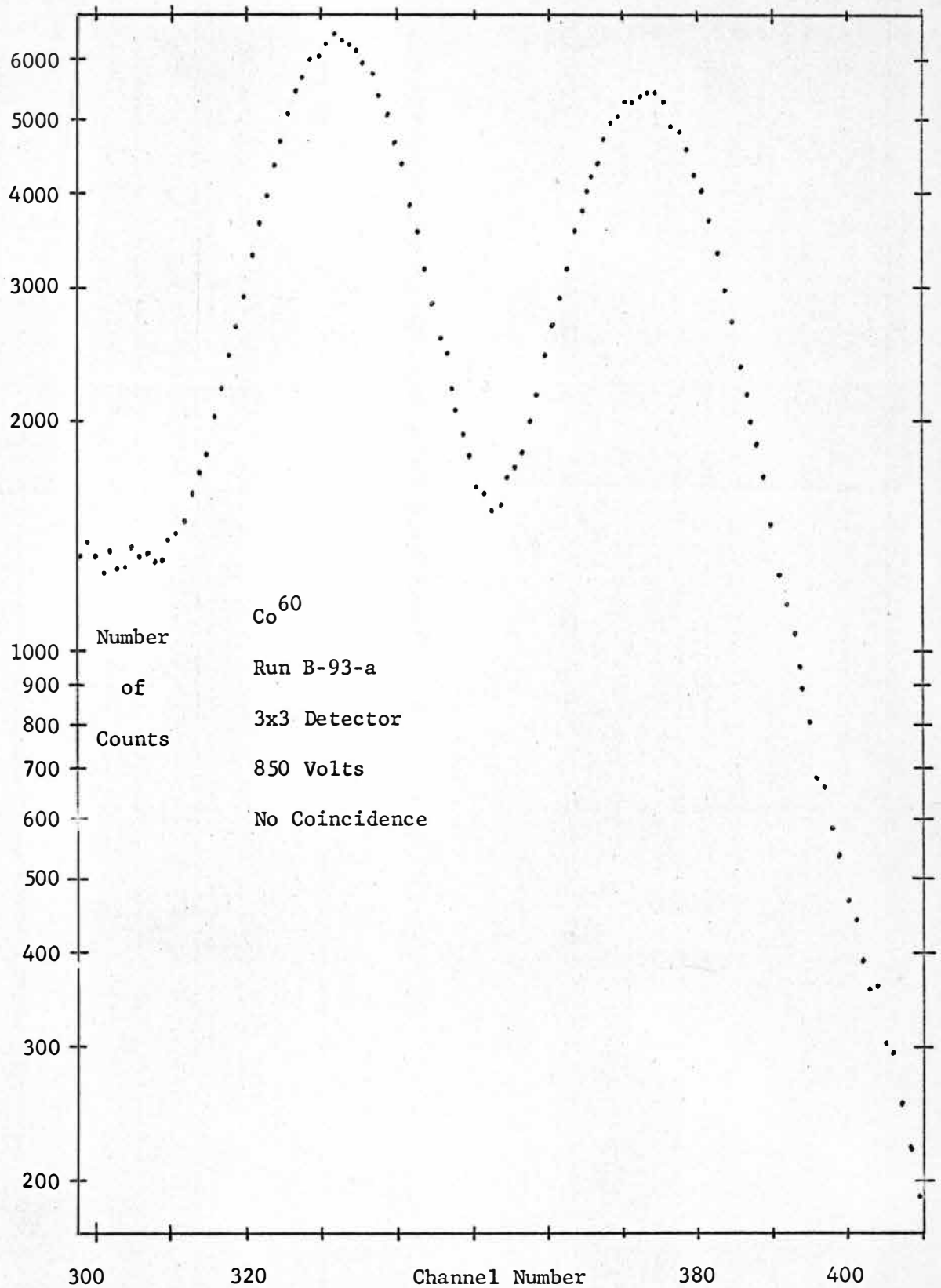
6000
5000
4000
3000
2000
1000
900
800
700
600
500
400
300
200
Number
of
Counts
Co60
Run B-93-a
3x3 Detector
850 Volts
No Coincidence
300
320
Channel Number
380
400

Fig. 13

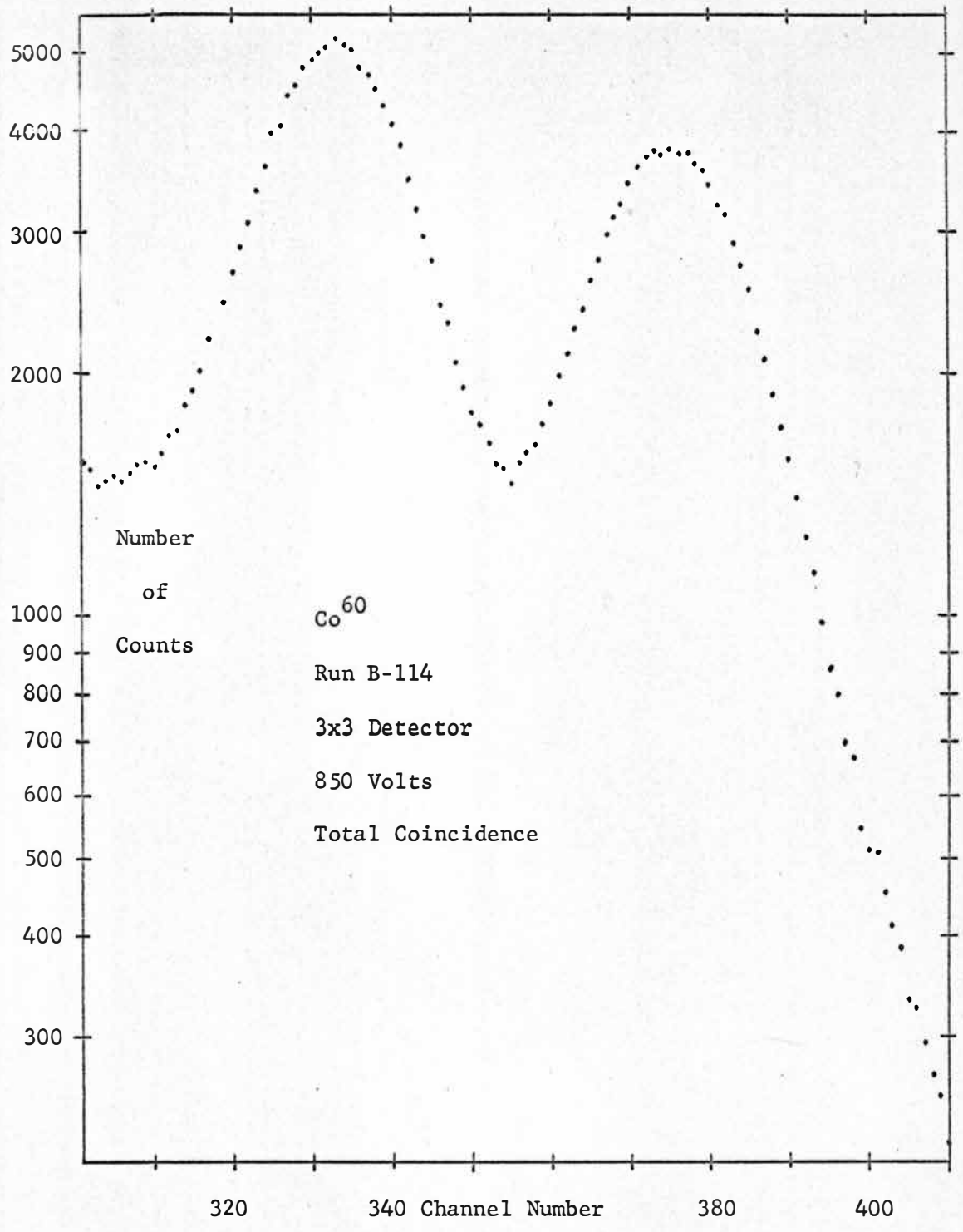
5000
4000
3000
2000
1000
900
800
700
600
500
400
300
Number
of
Counts
Co60
Run B-114
3x3 Detector
850 Volts
Total Coincidence
320
340
Channel Number
380
400

Fig. 14

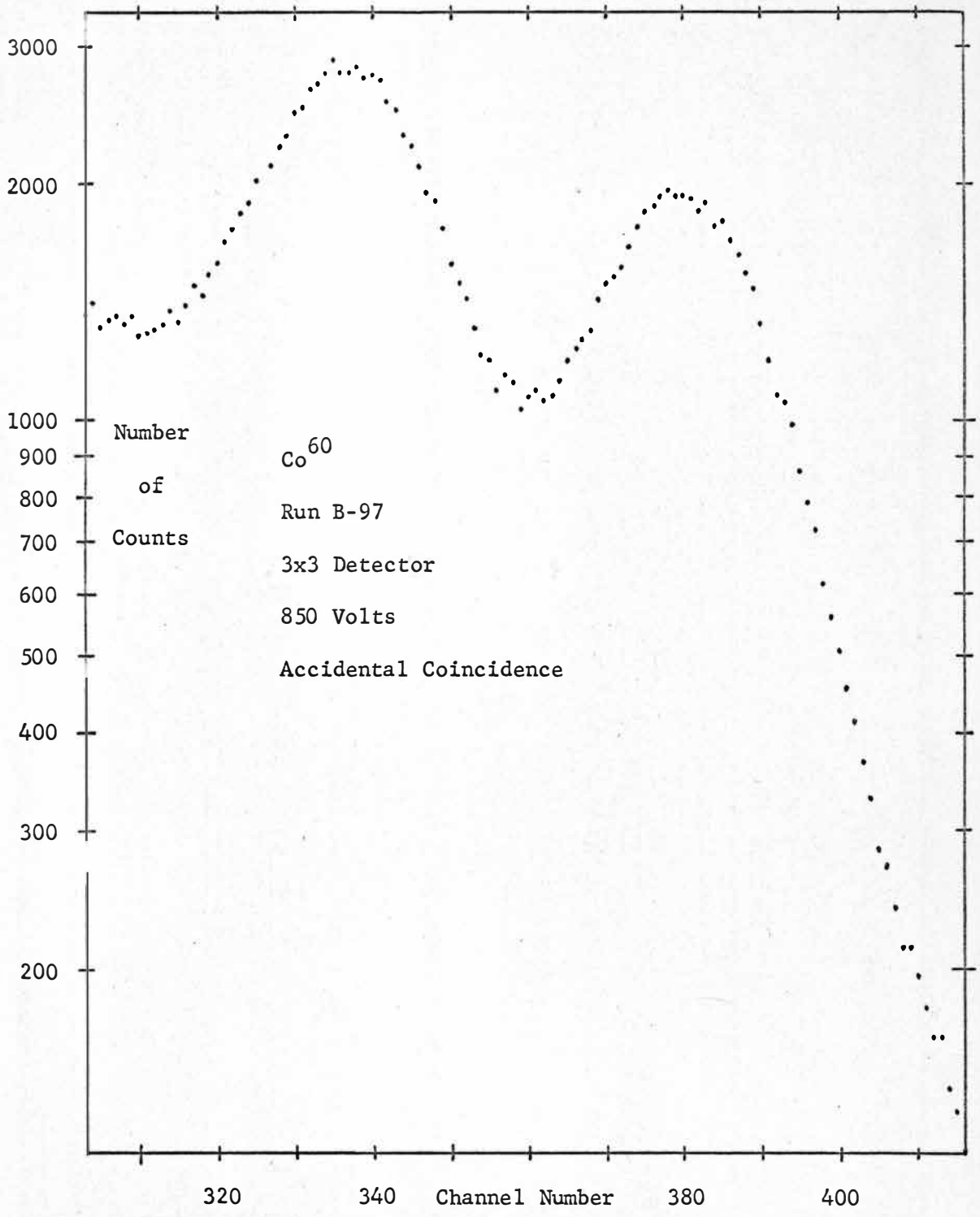
3000
2000
1000
900
800
700
600
500
400
300
200
Number
of
Counts
Co60
Run B-97
3x3 Detector
850 Volts
Accidental Coincidence
320
340
Channel Number
380
400

Fig. 15

true coincidence were straddled by the window thereby reaching their maxima while the coincidence pulse was positive. The signals that were in coincidence only accidentally were not necessarily straddled by the window. It is probable that their maximum while the window was open was not their point of greatest voltage amplitude. Their maximum might have come while the window was closed, and therefore they would have been stored in a lower channel number.

Net coincidence spectrum. Fig. 16 is a spectrum made by subtracting graphically an accidental coincidence spectrum from a total coincidence spectrum. This net coincidence spectrum is indistinguishable from a spectrum taken with no coincidence.

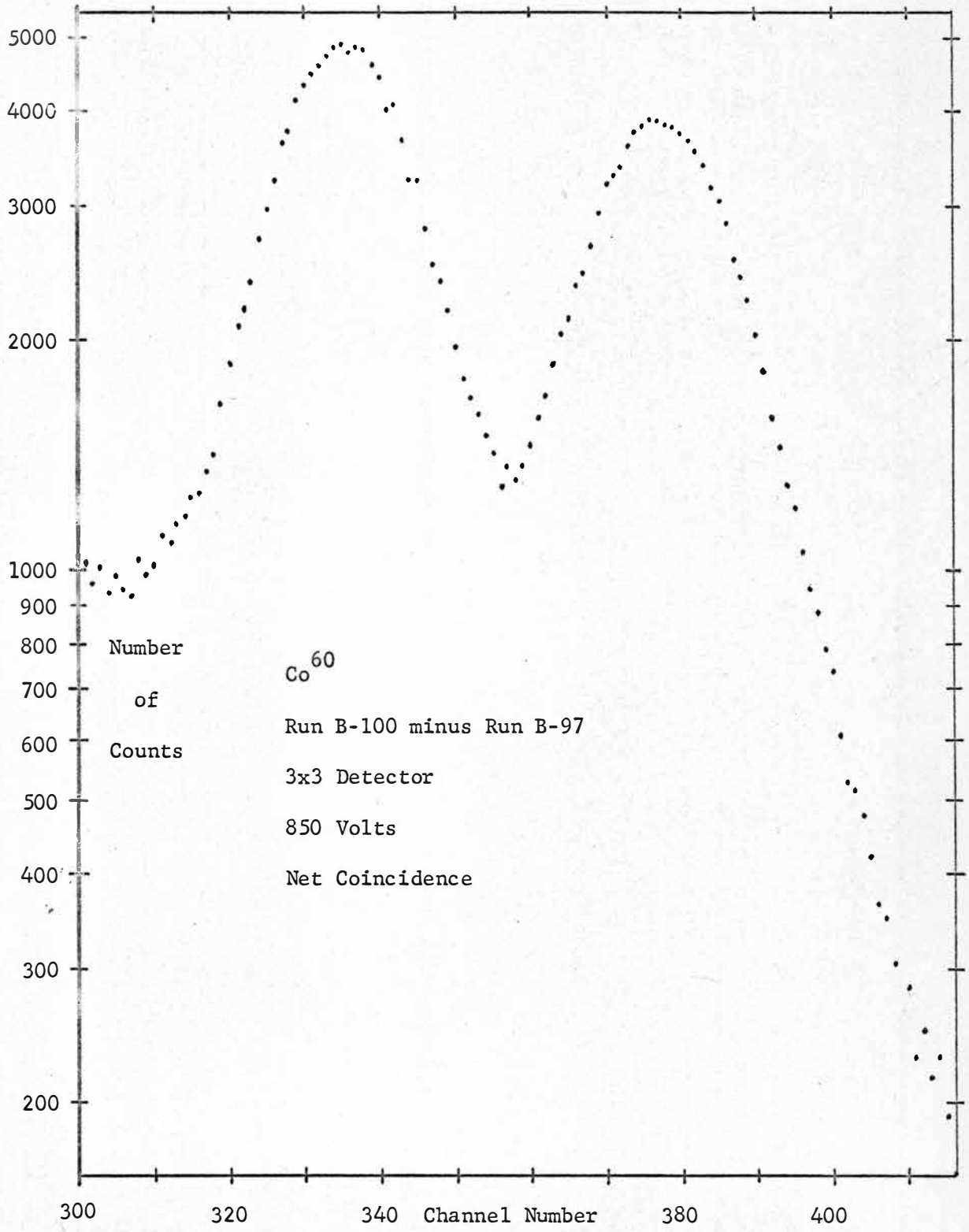
5000
4000
3000
2000
1000
900
800
700
600
500
400
300
200
Number
of
Counts
Co60
Run B-100 minus Run B-97
3x3 Detector
850 Volts
Net Coincidence
300
320
340
Channel Number
380
400

Fig. 16

II. Method of Counting

Experimental method. Since radioactive decay is a random process, the repeated measurements of a counting rate have a statistical distribution. Using the appropriate statistics, if the number of gamma rays counted in a certain interval is N, then the mean deviation for this measurement is $\sqrt{N}$. It is advantageous to have as many counts as possible, since the larger N is, the smaller the ratio $\frac{\sqrt{N}}{N}$ becomes.

The following notation will be used:

(a) The source strength, i.e., the number of disintegrations per second, is noted by M.

(b) The detection efficiencies of the 2x2 and 3x3 crystals are designated ϵ_1 and ϵ_2 respectively.

(c) The solid angles subtended by the 2x2 and 3x3 crystals are noted α_1 and α_2 respectively.

(d) The resolving time of the coincidence circuit is designated by π.

The true coincidence counting rate is proportional to $M\epsilon_1\alpha_1\epsilon_2\alpha_2$. The accidental coincidence counting rate is proportional to $M^2\epsilon_1\alpha_1\epsilon_2\alpha_2\pi$. It should be noted that the absolute efficiency of the crystals is given by $\epsilon_1\alpha_1$ and $\epsilon_2\alpha_2$ for the 2x2 and 3x3 detectors respectively.

A large number of counts, which is desirable for a precise measurement, may be obtained in the following manner: (a) counting over a large energy range; (b) making source strength large; (c) making α_1 and/or α_2 large; (d) counting for a long period of time.

For angular correlations, the direction of propagation of each gamma ray is of interest. Detection of gamma rays in one direction limits the energy range that can be counted over, since low energy scattered gamma rays must not be counted because their direction is not determined by the position of the counter. The source strength is limited by the fact that accidental coincidences become very important, and the net coincidences are therefore made more uncertain. The solid angles subtended by the counter can be made large by placing the crystals close to the source. However, usable solid angles are limited by the fact that the direction of the detected gamma ray must be known and the closer a crystal is to the source, the larger is the range of angles from which it will accept gamma rays. The length of time for which the gamma rays can be counted is limited by the fact that the phototubes tend to produce a drift in gain, which spreads the photopeaks and degrades resolution.

Optimum values. As a result of preliminary measurements, the following compromise values were chosen. The 3x3 was placed 10.0 cm away from the source. The 2x2 was located 6.0 cm from the source. The energy range selected to sum over was from 1.10 MeV to 1.45 MeV. The length of each run was approximately ten hours. With a source strength of 3.5 μC, the ratio of true coincidences to accidental coincidences was about 2 to 1. With a source strength of 5.0 μC, the ratio was about 1 to 1.

Centering of the sample. Preliminary work showed that optimum source strength was about 4 μC. The source was mounted on the table in such a manner that the source to detector distances would remain constant for different angles between the detectors. Since the source did not rotate with the 2x2 movable crystal, the distance between the source and the 3x3 stationary detector was not affected by rotating the 2x2 detector to different positions. For the distance between the source and the 2x2 movable detector to remain constant as the 2x2 detector rotated, it was imperative for the source to be on the axis of rotation. The method used to center the source was to make the window counting rate constant for all positions of the 2x2 detector. The window counting rate was recorded by the seven digit scaler.

Recording of data. Upon the completion of a run, the following data were recorded: a complete coincidence spectrum; the length of time of the run to the nearest second; and the number of times the window opened. Since the length of each run was about ten hours, the length of the run was accurate to within one twentieth of one percent. With the window counting rate being at least 70,000 counts per minute, the number of openings of the window was accurate to within one hundredth of one percent. The spectrum was then graphed on semi-log paper and the peaks located to the nearest tenth of a channel. The peaks were located by pinpointing the midpoint of a peak at half of its maximum. The channel in which this peak fell

drifted slightly from run to run due to inherent drift in the stability of the photomultiplier tube.

Summing of counts in photopeak. Since channel 0 corresponded to zero energy, any drift in overall gain could be interpreted as a change in the energy that each channel represented. Run B-77 was arbitrarily picked as a standard. The peaks in B-77 fell in channels 336.0 and 378.3. It was decided to count 102 channels, from channel 312 through 413. The total number of counts within this range was 430,462. The coincidence window opened 48,091,000 times.

As an example of the interpretation of a spectrum, run B-114 is calculated below. First the spectrum was graphed and the peaks located to be in channels 322.0 and 362.6. Since the photopeaks of γ_1 and γ_2 fall in lower channels than they did in run B-77, each channel in run B-114 represents a greater amount of energy. Therefore, to count over the same energy range as was counted over in run B-77, fewer channels must be counted. Working out the proportion (336.0 is to 322.0 as 102.0 is to x, so x = 97.7), 97.7 channels on this scale correspond in energy to 102.0 channels on the B-77 spectrum. On the B-77 spectrum, the first of the channels counted was located 24.0 channels below the midpoint of the 1.17 MeV peak. In run B-114, the first counted channel should be only 23.0 channels below the lower peak, because 336.0 is to 322.0 as 24.0 is to 23.0. This means that for this run, 97.7 channels (starting with channel 299.0 and continuing through channel 396.7) should be summed. The total number of counts within this interval

is 270,572. The coincidence window opened 31,173,000 times. Normalizing the counts to 48,091,000 openings of the coincidence window gives 417,415 as the normalized total number of counts.

Calculations similar to the above were carried out on each run. Thus it was guaranteed that each run was summed over the same energy range. Each run was also normalized to 48,091,000 openings of the coincidence window. The reason the counts were normalized to the number of openings of the window rather than to a constant time interval was to correct for any slight drift in gain of the 2x2 crystal's phototube. A change in this gain would make a slightly different counting rate for the coincidence window.

CHAPTER V

RESULTS

I. Correction Factors

Anisotropy. The correlation function can be written as follows: $W(\theta) = 1+A_2P_2(\cos\theta)+A_4P_4(\cos\theta)$. Experimentally the coefficients A_2 and A_4 are determined by measuring $W(\theta)$ at a number of angles and then fitting by least squares the above polynomial to the points. A knowledge of coincidence counting rates at 90° and 180° is sufficient for the calculation of the anisotropy A.

$$A \equiv \frac{W(180^\circ)-W(90^\circ)}{W(90^\circ)}$$

Measured correlation function. Experimentally it is not possible to measure $W(\theta)$ directly since the counters subtend finite solid angles. Instead, the spread out correlation function $\langle W(\theta)\rangle$ is measured, because of the finite solid angles of the counters. The measured function can be written as follows: $\langle W(\theta)\rangle = K\left[1+A_2{*}P_2(\cos\theta)+A_4{*}P_4(\cos\theta)\right]$.[14] The measured coefficients are related to the true coefficients by the following:

$$A_2 = \frac{Q_o}{Q_2} A_2{*};\quad A_4 = \frac{Q_o}{Q_4} A_4{*};$$

where $Q_j = J_j{}^I J_j{}^{II}$ ($j = 0, 2,$ or 4)

and where $J_k{}^i = \int P_k(\cos\alpha)\epsilon^i(\alpha)\left|\sin\alpha\right|d\alpha.$

(i = I or II; $k = 0,2,$ or 4)

---

[14] J. S. Lawson, Jr., and H. Fraunfelder, Physical Review, Vol. 91, p. 649, (1953).

The relative angular efficiency of the 3x3 crystal is $\epsilon^{I}(\alpha)$, where α is the angle between the axis of the 3x3 crystal and a collimated beam of gamma rays. The relative angular efficiency of the 2x2 crystal is $\epsilon^{II}(\alpha)$, where α is the angle between the axis of the 2x2 crystal and a collimated beam of gamma rays.

Collimating a gamma ray beam. To facilitate the measurement of $\epsilon^{I}(\alpha)$, a beam of gamma rays from Co^{60} was collimated. Since gamma rays cannot be focused, collimation of a beam was accomplished by absorbing all the gamma rays being emitted by a source except those within a very small solid angle. The 2 mC source was surrounded on all sides by at least ten cm of lead bricks. A small 2 mm hole was drilled through two of the bricks. Upon alignment of the source behind the hole in these two bricks, a collimated pencil of gamma radiation emerged.

To verify that the radiation was collimated, the following measurements were made. A narrow counter was placed 66.0 cm from the last absorbing brick and rotated in 0.5^{o} steps about a 66.0 cm radius. A narrow counter was created by shielding all of the face of the 3x3 crystal except a vertical strip 0.5 cm wide. The results of these measurements showed that the beam had an angular spread of not greater than 1.5^{o}.

Measurement of the angular efficiency of the crystals. The angular efficiency $\epsilon^{I}(\alpha)$ was measured by determining the counting rate of the 3x3 crystal as a function of the angle α between the

axis of the crystal and the collimated beam of gamma rays. To determine this counting rate, the detector was rotated about a 10.0 cm radius in increments of 5^{o}. While the detector was in each position, a complete spectrum was recorded for 2.0000 live minutes. The total number of pulses recorded between 1.10 MeV and 1.45 MeV was then summed. Since the total number of counts for each angle α was recorded for exactly equal time intervals, $\epsilon^{I}(\alpha)$ can be represented by a plot of the total counts vs. the angle α.

The angular efficiency $\epsilon^{II}(\alpha)$ was determined in a similar manner. The 2x2 crystal was rotated about the collimated beam of gamma rays in increments of 5^{o}. The 2x2 crystal was rotated about a 6.0 cm radius. Fig. 17 shows the result of the measurement of $\epsilon^{I}(\alpha)$. Fig. 18 shows the result of the measurement of $\epsilon^{II}(\alpha)$.

Graphical calculation of the angular efficiencies of the crystals. The angular efficiency $\epsilon^{I}(\alpha)$ can also be calculated geometrically as shown in Fig. 19. For angles greater than α_2, only background radiation is recorded by the crystal. For angles less than α_1, the counting rate has a broad maximum and is almost independent of α since the gamma rays within this wedge traverse almost equal thicknesses of the crystal. The counting rate for angles between α_1 and α_2 can be obtained by using $I = I_o e^{-\beta x}$, where β for sodium iodide is 0.081 cm^{-1} for gamma rays in the

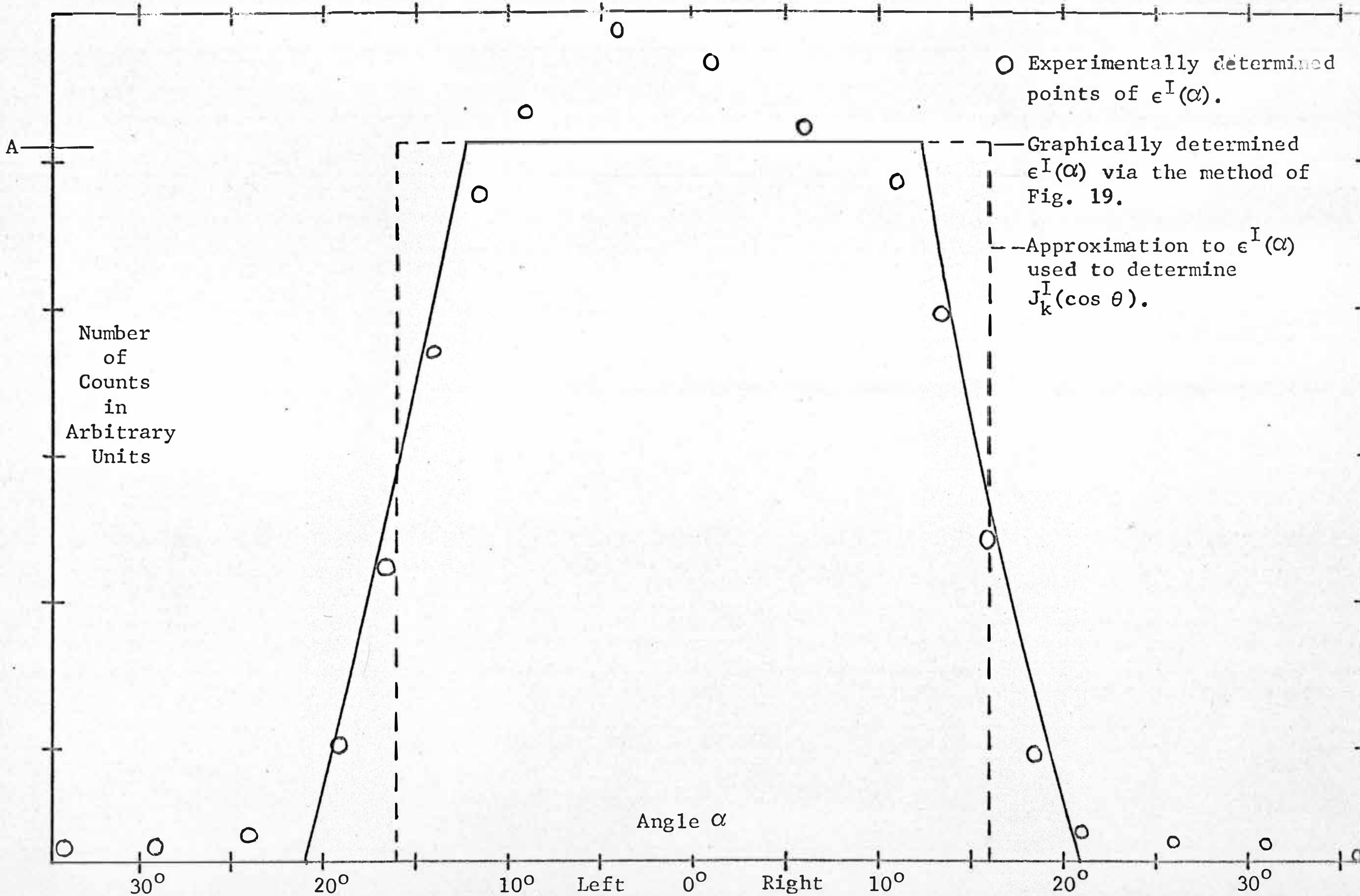
Experimentally determined points of $\epsilon^{I}(\alpha)$.
Graphically determined $\epsilon^{I}(\alpha)$ via the method of Fig. 19.
Approximation to $\epsilon^{I}(\alpha)$ used to determine $J_k^I(\cos\theta)$.
A
Number of Counts in Arbitrary Units
Angle α
30°
20°
10°
Left
0°
Right
10°
20°
30°

Fig. 17

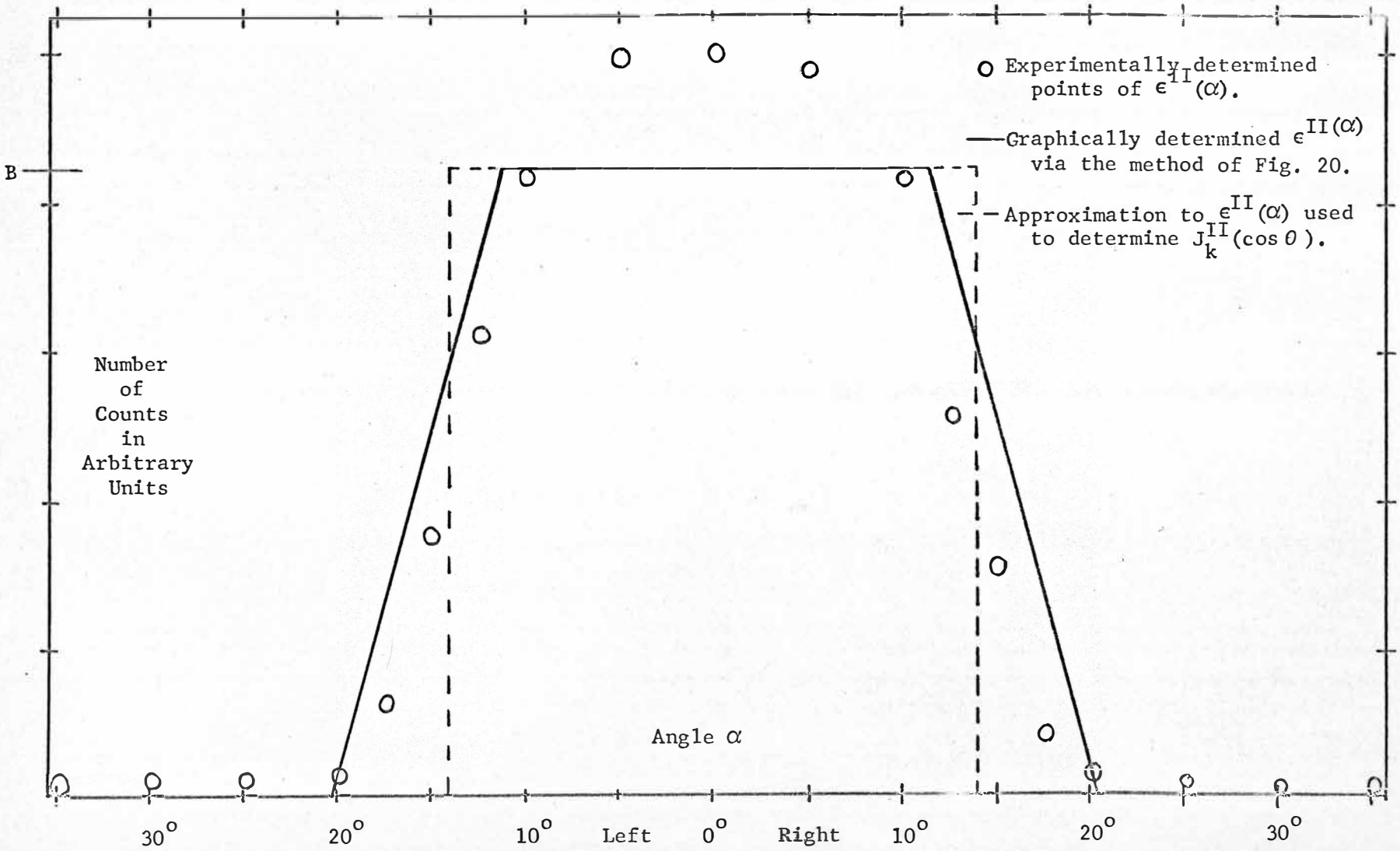
Experimentally determined points of $\epsilon^{II}(\alpha)$.
Graphically determined $\epsilon^{II}(\alpha)$ via the method of Fig. 20.
Approximation to $\epsilon^{II}(\alpha)$ used to determine $J_k^{II}(\cos\theta)$.
B
Number of Counts in Arbitrary Units
Angle α
30°
20°
10°
Left
0°
Right
10°
20°
30°

Fig. 18

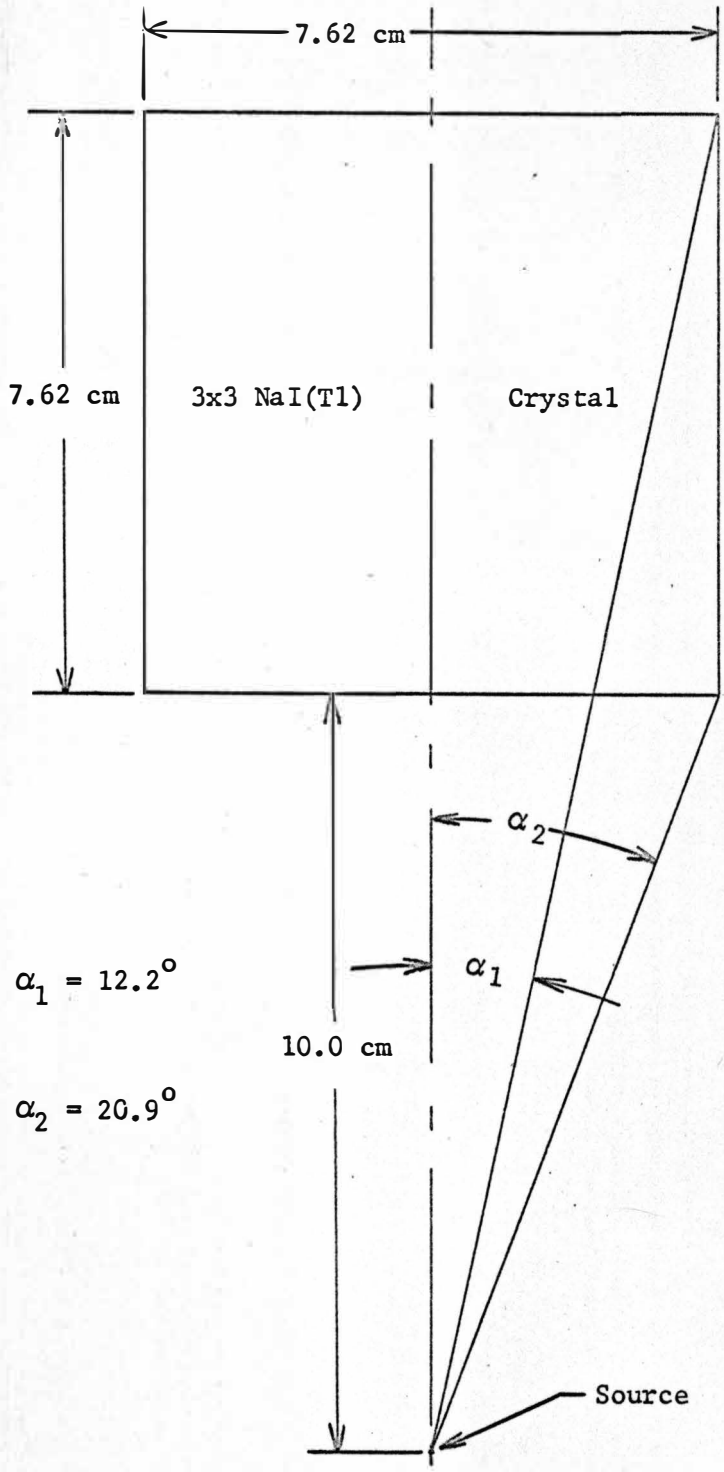
7.62 cm
7.62 cm
3x3 NaI(Tl)
Crystal
α_2
α_1
$\alpha_1 = 12.2^o$
10.0 cm
$\alpha_2 = 20.9^o$
Source

Fig. 19

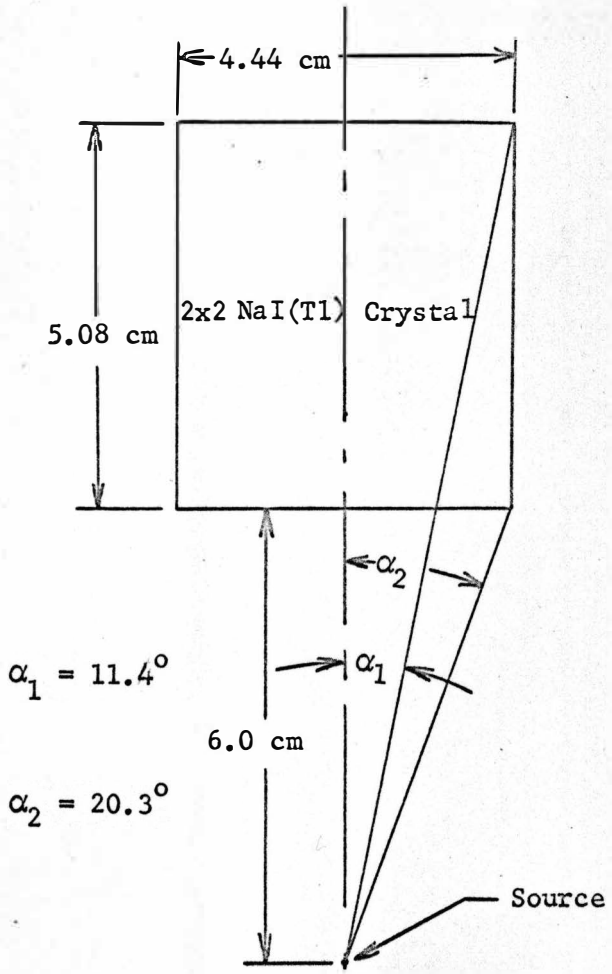
4.44 cm
5.08 cm
2x2 NaI(Tl) Crystal
α_2
α_1
$\alpha_1 = 11.4^\circ$
6.0 cm
$\alpha_2 = 20.3^\circ$
Source

Fig. 20

energy range 1.17 to 1.33 MeV.[15] A similar calculation for $\epsilon^{II}(\alpha)$ appears in Fig. 20. It should be noted that although the crystal is designated as a 2x2, its actual dimensions are 1 3/4 inches in diameter by 2 inches thick.

Correction factor results. Use of the measured angular efficiencies, and an evaluation of the integral determined the following coefficients:

$$J_0^I = 0.0775A \qquad J_0^{II} = 0.0594B$$

$$J_2^I = 0.0730A \qquad J_2^{II} = 0.0568B$$

$$J_4^I = 0.0633A \qquad J_4^{II} = 0.0510B.$$

Calculation of the ratios of these yielded the following:

$$\frac{J_2^I}{J_0^I} = 0.942 \qquad \frac{J_2^{II}}{J_0^{II}} = 0.956$$

$$\frac{J_4^I}{J_0^I} = 0.817 \qquad \frac{J_4^{II}}{J_0^{II}} = 0.859.$$

---

[15] G. R. White, "X-ray Attenuation Coefficients from 10 KeV to 100 MeV," National Bureau of Standards (U. S.) Report 1003, (1952).

These ratios have been calculated by West[16] according to the method of Rose[17] and are shown below:

(For a) (3x3)	$\frac{J_2}{J_0} = 0.908$	(For a) (2x2)	$\frac{J_2}{J_0} = 0.912$
	$\frac{J_4}{J_0} = 0.712$		$\frac{J_4}{J_0} = 0.722.$

It should be noted that the coefficients determined in this experiment are consistently closer to unity than those calculated by West. This is predictable because the calculated coefficients were derived for gamma rays which interact with the crystal by any of the three modes (photoelectric effect, Compton effect, or pair production). These experimentally determined coefficients were measured for only those gamma rays which gave all of their energy to the crystal.

Measured coefficients. The following coefficients in the Legendre polynomial expansion of $W(\theta)$ were evaluated by the use of the tables of Biedenharn:[1]

$$A_0 = 1.0000 \qquad A_2 = 0.1020 \qquad A_4 = 0.0091.$$

---

[16] H. I. West, Jr., "Angular Correlation Factors via the Method of Rose," University of California Radiation Laboratory, (Livermore,) Report UCRL-5451 (1959).

[17] M. E. Rose, Physical Review, Vol. 91, p. 610, (1953).

[1] L. C. Biedenharn and M. E. Rose, Reviews of Modern Physics, Vol. 25, p. 3, (1953).

By the use of these coefficients, the anisotropy was determined to be $A = 0.1667$.

By the application of the experimentally determined correction factors, the following coefficients which would be measured experimentally were obtained,

$$A_0^* = 1.0000 \qquad A_2^* = 0.0920 \qquad A_4^* = 0.0064.$$

By the use of these coefficients, the measured anisotropy was calculated to be $A^* = 0.1480$.

II. Error Analysis

Propagation of errors. As an example of the propagation of errors, a value of the anisotropy is calculated below. Run B-92, which had 541,866 ± 658 counts in its photopeaks, was used to determine the total number of coincidences at 180°. Run B-91, which had 415,561 ± 634 counts, was used to determine the total coincidences at 270°. Run B-97, which had 162,735 ± 418 counts, was used to determine the number of accidental coincidences at 180°. Run B-98, which had 162,709 ± 485 counts, was used to determine the number of accidental coincidences at 270°. True coincidences are given by the total number of coincidences minus the number of accidental coincidences.

The following were obtained by the subtraction of the accidentals from the totals: $W(180^\circ) = 289,131 \pm 780$; $W(90^\circ) = 252,852 \pm 793$, and $A^* = 0.1435 \pm 0.0060$.

It should be noted that although the counting rates are each accurate to within less than 0.3%, the anisotropy is certain to within only 4.2%.

III. Data

Fig. 21 shows the number of total coincidence counts recorded from the 3.5 μC source at various angles between the two detectors. The number of counts plotted on the ordinate has been summed and normalized via the method of Chapter IV. Fig. 22 shows the normalized number of counts recorded with the 5.0 μC source. Fig. 23 and Fig. 24 display the normalized number of accidental coincidence counts recorded from each of the two sources.

Discrepancy in coincidence counting rates at 270° and 90°.

The angle θ was measured from the 3x3 stationary crystal to the 2x2 crystal in the counterclockwise direction as viewed from the top. The number of coincidence counts recorded at $\theta = 90^{\circ}$ was consistently higher than with $\theta = 270^{\circ}$. Possible explanations for this discrepancy are the following: (a) small angle scattering from the surroundings; (b) slight bending by the earth's magnetic field of the electrons in the photomultiplier tubes, thereby changing the gain; (c) an asymmetry in the amount of absorption of the gamma rays by the source holder; (d) an asymmetry in the efficiency of the 3x3 stationary crystal.

In an effort to remedy this discrepancy in counting rates, a number of adjustments were made in the arrangement of the detectors.

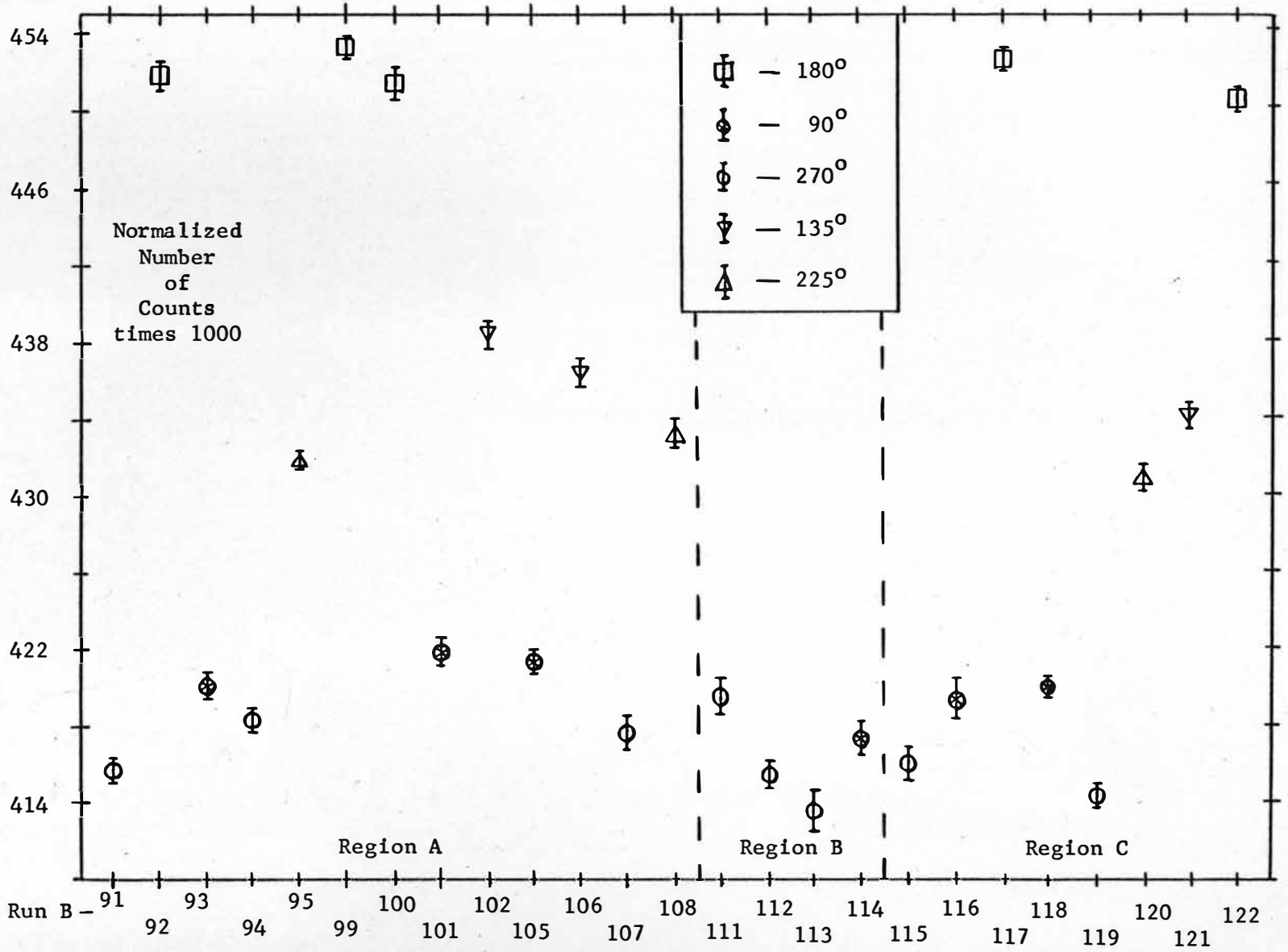
454
446
438
430
422
414
Normalized
Number
of
Counts
times 1000
180°
90°
270°
135°
225°
Region A
Region B
Region C
Run B –
91
92
93
94
95
99
100
101
102
105
106
107
108
111
112
113
114
115
116
117
118
119
120
121
122

Fig. 21

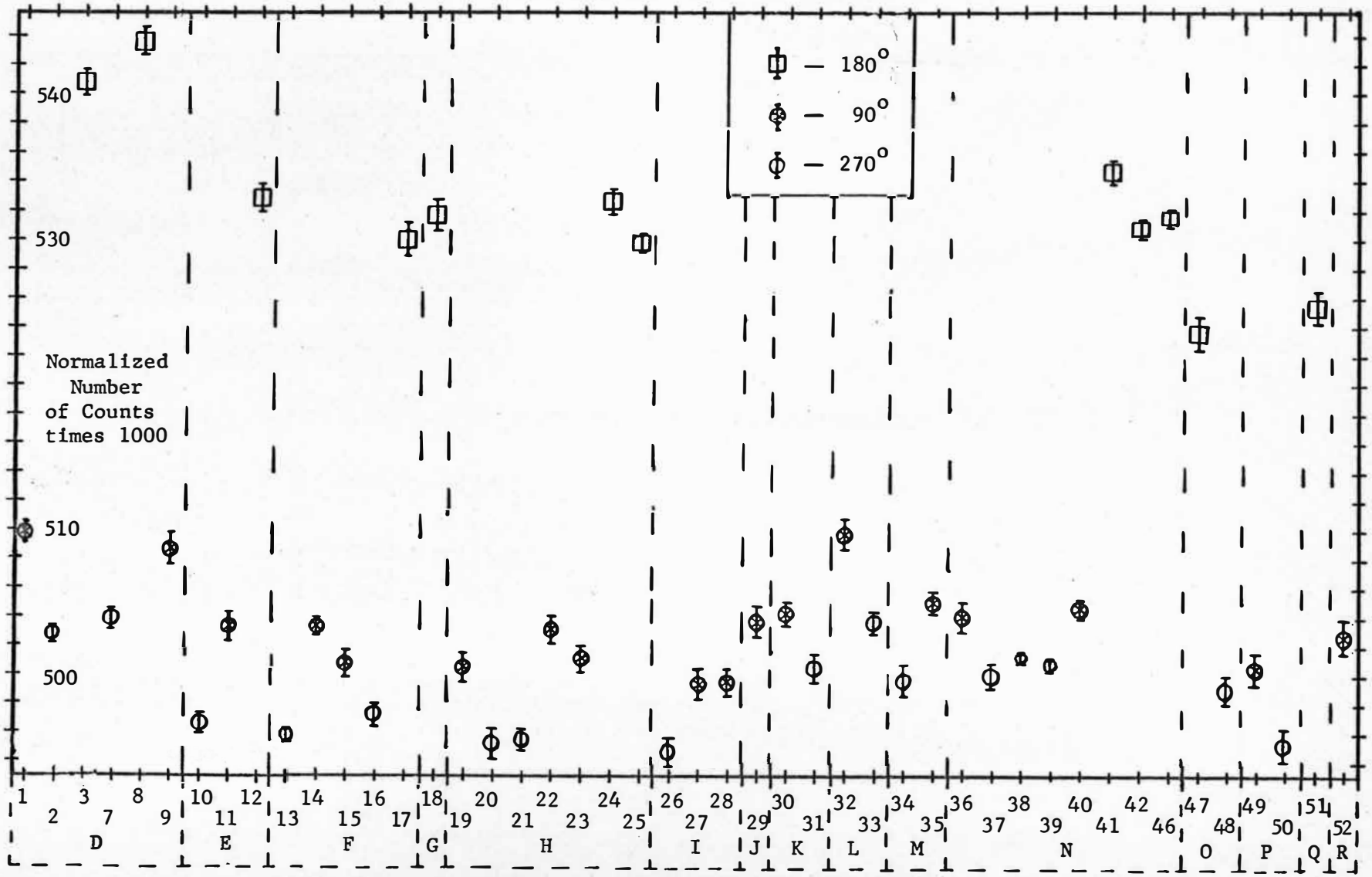
Φ — 180°
Φ — 90°
Φ — 270°
540
530
510
500
Normalized
Number
of Counts
times 1000
1 2 3 7 8 9 10 11 12 13 14 15 16 17 18 19 20 21 22 23 24 25 26 27 28 29 30 31 32 33 34 35 36 37 38 39 40 41 42 46 47 48 49 50 51 52
D E F G H I J K L M N O P Q R

Fig. 22.

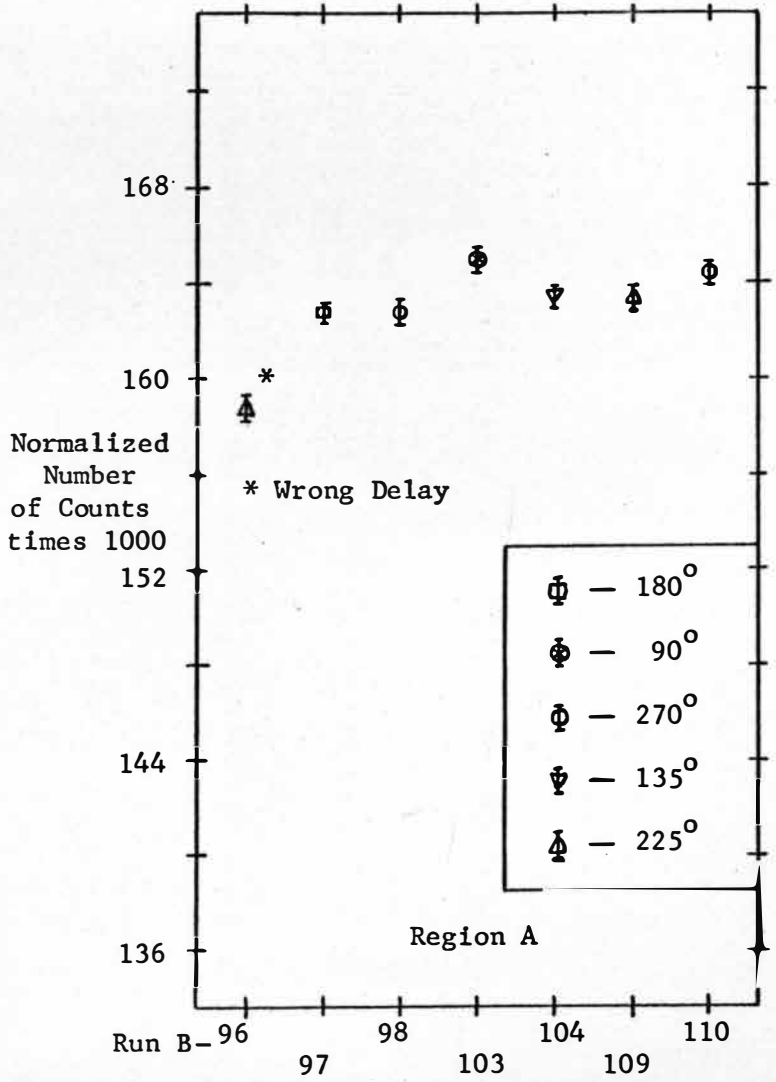
168
160
152
144
136
Normalized
Number
of Counts
times 1000
* Wrong Delay
Φ — 180°
Φ — 90°
Φ — 270°
Φ — 135°
Φ — 225°
Region A
Run B— 96 97 98 103 104 109 110

Fig. 23.

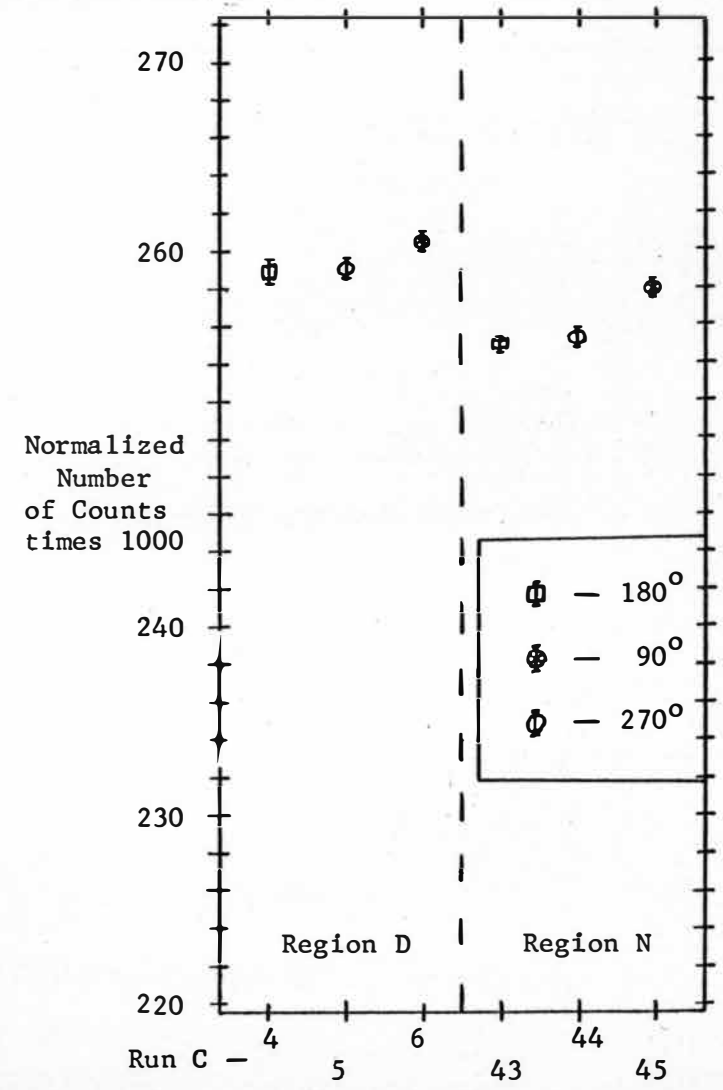
270
260
240
230
220
Normalized
Number
of Counts
times 1000
Φ — 180°
Φ — 90°
Φ — 270°
Region D
Region N
Run C — 4 5 6 43 44 45

Fig. 24.

These adjustments are shown by the different regions in Fig. 21 and Fig. 22. The effects of small angle scattering and bending of electrons by the earth's magnetic field were reversed by rotating the angular correlation table by 180°. An asymmetry in the amount of absorption by the source holder was eliminated by replacing the source and source holder. An asymmetry in the efficiency of the 3x3 detector was checked by turning the detector upside down.

Explanation of the regions of Fig. 21 and Fig. 22. The following is an explanation of the variations made in the arrangement of the detectors.

In region A, the 3x3 stationary detector was pointed west.

In region B, the angular correlation table was rotated 180° (i.e., the 3x3 detector was pointed east).

In region C, the 3x3 crystal remained pointed east, but the sample was re-centered.

In region D and all subsequent regions, the 5.0 μC source was used. The 3x3 detector remained pointed east.

In region E and all subsequent regions, the 3x3 crystal was turned upside down. However, it remained pointed east.

In region F, the angular correlation table was rotated 45° (i.e., the 3x3 detector was pointed northeast).

In region G, the angular correlation table was again rotated 45° so that the 3x3 pointed north.

In region H, the angular correlation table was rotated back 45° so that the 3x3 crystal again pointed northeast. The sample was rotated 180° in its holder.

In region I, the sample was re-centered, but the table was not rotated.

In region J, the setting of the window was changed slightly by changing the gain on the linear amplifier connected to the differential discriminator. A magnetic shield was also added to the 6292 photomultiplier tube on which the 2x2 movable detector was mounted. The table was not rotated.

With the 2x2 detector right side up (as it was through region J), the gain of the 6292 photomultiplier tube was unaffected by the orientation of the 2x2 crystal. Turning the detector upside down caused the gain to vary markedly at different positions. After placing a magnetic shield around the 6292 tube, the gain was again independent of the orientation of the detector.

In region K, the 2x2 movable detector was turned upside down. The angular correlation table was not rotated.

In region L, the 2x2 detector was turned right side up again. The table was not rotated (i.e., the 3x3 stationary crystal was still pointed northeast); however, the sample was re-centered.

In region M, the only change was that the sample was re-centered.

In region N, the angular correlation table was rotated by 180° so the 3x3 stationary detector pointed southwest.

In region O, the angular correlation table was rotated by 45° (i.e., the 3x3 crystal pointed south). The source was also re-centered.

In region P, the setting of the window was slightly changed by adjusting the value of E on the differential discriminator.

In region Q, the setting of the window was again slightly changed by adjusting E.

In region R, the setting of the window was again slightly changed by adjusting E.

Table I shows the values of the measured anisotropy A*. The weighted average of these different values is given by

$$A^* = 0.1384 \pm 0.0077.$$

Reg.	$\frac{W(180^\circ) - W(90^\circ)}{W(90^\circ)}$	$\frac{W(180^\circ) - W(270^\circ)}{W(270^\circ)}$
A	0.1303 ± 0.0061	0.1415 ± 0.0090
C	0.1329 ± 0.0069	0.1510 ± 0.0088
D	0.1403 ± 0.0086	0.1603 ± 0.0102
E	0.1286 ± 0.0082	0.1533 ± 0.0085
F	0.1237 ± 0.0084	0.1424 ± 0.0081
H	0.1305 ± 0.0082	0.1525 ± 0.0095
N	0.1254 ± 0.0102	0.1302 ± 0.0103
Weighted Average	0.1309 ± 0.0054	0.1456 ± 0.0101

Table I.

BIBLIOGRAPHY

F. Ajzenberg-Selove, Nuclear Spectroscopy (Academic Press Inc., New York, 1960).

J. R. Bell, and P. R. Cheever, Nucleonics, Vol. 21, p. 58, (July 1963).

L. C. Biedenharn and M. E. Rose, Reviews of Modern Physics, Vol. 25, p. 3, (1953).

M. Deutsch, L. G. Elliott, and A. Roberts, Physical Review, Vol. 68, p. 193, (1945).

H. Ferentz and N. Rosenzweig, Argonne National Laboratory Report 5324, (1954).

J. B. Garg and N. H. Gale, Nuovo Cimento, Vol. 16, p. 1014, (June 1960).

R. L. Heath, "Scintillation Spectrometry: Gamma-Ray Spectrum Catalogue," Phillips Petroleum Co. Report IDO-16408, (1957).

E. D. Klema and F. K. McGowan, Physical Review, Vol. 91, p. 616, (1953).

J. S. Lawson, Jr., and H. Fraunfelder, Physical Review, Vol. 91, p. 649, (1953).

Nuclear Data Sheets, Vol. 2, (1961).

Reviews of Modern Physics, Vol. 30, p. 631, (1958).

M. E. Rose, Physical Review, Vol. 91, p. 610, (1953).

E. Segre, Experimental Nuclear Physics (John Wiley and Sons, New York, 1959).

A. K. Sen Gupta and D. M. Van Patter, Physical Letters, Vol. 3, p. 355, (February 1963).

K. Siegbahn, Beta- and Gamma-Ray Spectroscopy (Interscience Publishers Inc., New York, 1955).

R. M. Steffen, Advances in Physics, Vol. 4, p. 293, (1955).

M. A. Waggoner, Physical Review, Vol. 82, p. 906, (1951).

K. Way, et. al., "Nuclear Level Schemes," A = 20 - A = 92 Atomic Energy Commission Report TID-5300, (1955).

H. I. West, Jr., "Angular Correlation Factors via the Method of Rose," University of California Radiation Laboratory (Livermore,) Report UCRL-5451, (1959).

G. R. White, "X-ray Attenuation Coefficients from 10 KeV to 100 MeV, National Bureau of Standards (U. S.) Report 1003, (1952).

E. A. Wolicki, et. al., "Calculated Efficiencies of NaI Crystals," U. S. Naval Research Laboratory Report NRL-4833, (1956).